Nonclinical Characterization of the HIF-Prolyl Hydroxylase Inhibitor Roxadustat, a Novel Treatment for Anemia of Chronic Kidney Disease

Ughetta del Balzo*, Pierre E. Signore*, Gail Walkinshaw, Todd W. Seeley, Mitchell C. Brenner, Qingjian Wang, Guangjie Guo, Michael P. Arend, Lee A. Flippin, F. Aisha Chow, David C. Gervasi, Christian H. Kjaergaard, Ingrid Langsetmo, Volkmar Guenzler, David Y. Liu, Steve J. Klaus, Al Lin, and Thomas B. Neff.

Primary laboratory of origin: FibroGen, Inc., 409 Illinois Street, San Francisco, CA 94158 USA

Affiliations: FibroGen, Inc., 409 Illinois Street, San Francisco, CA 94158 USA (U.d.B, P.E.S., G.W., T.W.D., M.C.B., Q.W., G.G., M.P.A., L.A.F., F.A.C., D.C.G., C.H.K, I.L., V.G., D.Y.L., S.J.K., A.L., T.B.N.)

*Contributed equally to the study.

Running title: Nonclinical Profile of Roxadustat for Anemia

Corresponding Author: Ughetta del Balzo

FibroGen, Inc.

409 Illinois Street

San Francisco, CA 94158 USA

Telephone: 415 978 1852

Email: udelbalzo@fibrogen.com

Number of text pages: 47

Number of tables: 1

Number of figures: 9

Number of references: 64

Number of words in abstract: 248

Number of words in introduction: 745

Number of words in discussion: 1557

List of non-standard abbreviations:

αKG   α-ketoglutarate

ACD   anemia of chronic disease

BPE   bovine pituitary extract

BUN   blood urea nitrogen

CKD   chronic kidney disease

DCYTB	duodenal cytochrome b
Dcytb	gene coding for DCYTB protein
DMEM	Dulbecco's Modified Eagle's Medium
DMSO	dimethyl sulfoxide
DMT1	divalent metal transporter 1
Dmt1	gene coding for DMT1 protein
EGF	epidermal growth factor
EPO	erythropoietin
ESA	erythropoiesis-stimulating agents
FBS	fetal bovine serum
FIH	factor inhibiting HIF
GM-CSF	granulocyte-macrophage colony-stimulating factor
Hamp	gene coding for hepcidin
HIF	hypoxia-inducible factor
HIF-PH	HIF prolyl hydroxylase
IL	interleukin
LC-MS	liquid chromatography-mass spectrometry
MCHC	mean corpuscular hemoglobin concentration
MIP	macrophage inflammatory protein
MCV	mean corpuscular volume
PBS	phosphate-buffered saline
PCR	polymerase chain reaction
PG-PS	peptidoglycan-polysaccharide

PHD	prolyl hydroxylase
PK	pharmacokinetic
qRT-PCR	quantitative real-time polymerase chain reaction
Slc11a2	gene coding for DMT1 protein
TNF	tumor necrosis factor
WBC	white blood cells

Section assignment: Drug Discovery and Translational Medicine

ABSTRACT

Anemia of chronic kidney disease (CKD) is a multifactorial disorder caused by impaired erythropoietin (EPO) production and altered iron homeostasis associated with inflammation. Hypoxia-inducible factor (HIF) is a transcription factor that stimulates erythropoiesis via a coordinated response involving increased EPO production and enhanced iron availability for hemoglobin synthesis. HIF degradation is regulated by HIF-prolyl hydroxylase (PH) enzymes. We hypothesized that roxadustat, an orally available small-molecule inhibitor of HIF-PH, would increase EPO production and promote erythropoiesis in animal models of anemia. In cells, roxadustat increased both HIF-1α and HIF-2α proteins, leading to an increase in EPO production, even in the presence of EPO-suppressing inflammatory cytokines. Roxadustat administered intermittently to healthy rats and cynomolgus monkeys increased circulating EPO levels, reticulocytes, blood hemoglobin, and hematocrit in a dose-dependent manner. Roxadustat corrected anemia in a rat model of CKD after 5/6th nephrectomy and in a rat model of anemia of inflammation with impaired iron metabolism induced by peptidoglycan polysaccharide (PG-PS). In the PG-PS model, roxadustat significantly decreased hepatic expression of hepcidin, a hormone responsible for iron sequestration and functional iron deficiency, and increased expression of two genes involved in duodenal iron absorption: divalent metal transporter 1 and duodenal cytochrome b. In conclusion, by activating the HIF pathway roxadustat increased EPO production, elevated hemoglobin, corrected anemia, and improved iron homeostasis. The coordinated erythropoietic response stimulated by roxadustat, involving both EPO

production and mobilization of iron stores, makes this compound a promising treatment

for anemia of CKD and anemia associated with functional iron deficiency.

Significance Statement

Roxadustat is a novel orally available small-molecule inhibitor of HIF prolyl hydroxylase enzymes that reversibly stabilizes HIF-α, thus activating transcription of HIF-dependent genes, including EPO and regulators of iron homeostasis. Activation of the HIF pathway by roxadustat induces erythropoiesis in healthy rats and monkeys, and corrects experimentally-induced anemia in rats. The coordinated erythropoietic response that increases EPO production and mobilizes iron stores makes roxadustat a promising treatment for anemia of CKD and anemia associated with functional iron deficiency.

Introduction

Anemia is a frequent and serious complication of chronic kidney disease (CKD) that affects millions of patients worldwide (Kassebaum et al, 2014; Stauffer and Fan, 2014; Thomas et al., 2008). Anemia of CKD contributes to decreased quality of life and increased risk of morbidity and mortality (Finkelstein et al., 2009; Thorp et al., 2009). Key factors responsible for anemia of CKD are a relative deficiency in erythropoietin (EPO) production and a decrease in iron availability for hemoglobin (Hb) synthesis (Babitt and Lin, 2012; Locatelli et al., 2017; Yilmaz et al., 2011). Currently, anemia of CKD is managed by iron supplementation and, in more severe cases, by administration of supraphysiologic doses of erythropoiesis-stimulating agents (ESAs), such as human recombinant EPO, in combination with adjuvant iron therapy (Biggar and Kim, 2017). However, some patients are hyporesponsive to ESAs and need even larger doses because of functional iron deficiency associated with inflammation (Yilmaz et al., 2011; MacDougall and Cooper, 2005; Adamson, 2009). High doses of ESAs increase the risk of serious adverse events, including death, myocardial infarction, congestive heart failure, and stroke (Szczech et al., 2008; Pfeffer et al., 2009). Thus, to effectively treat anemia of CKD, new therapies need to address both impaired EPO production and functional iron deficiency (Locatelli et al., 2017).

The observation that low blood oxygen levels lead to increased EPO production was made decades ago (Prentice and Mirand, 1961; Naets, 1963), but the transcription factors responsible for this hypoxic response were not identified until the 1990s (Semenza and Wang, 1992; Wang and Semenza, 1995; Wang et al., 1995; Tian et al., 1997). Since then, these hypoxia-inducible factors (HIFs) have been found to be part of

an oxygen-sensing pathway that is evolutionarily conserved among metazoans (Kaelin, 2005; Kaelin and Ratcliffe, 2008). HIFs function as heterodimers comprising an oxygen-regulated α-subunit and a constitutively expressed β-subunit. There are two major HIF-α isoforms, HIF-1α and HIF-2α, both of which dimerize with the same β-subunit to form functional HIF-1 and HIF-2 transcription factors, respectively. In the presence of oxygen, HIF-α subunits are hydroxylated on specific proline residues by a family of HIF prolyl hydroxylase (HIF-PH) enzymes comprising three isozymes: PHD1 (EGLN2), PHD2 (EGLN1), and PHD3 (EGLN3) (Kaelin and Ratcliffe, 2008; Myllyharju, 2013). This hydroxylation enables binding of the von Hippel-Lindau protein, a component of an E3 ubiquitin ligase, which ubiquitinates HIF-α to target it for proteasomal degradation. HIF-PH enzymes require α-ketoglutarate (αKG) and oxygen as co-substrates. Thus, when oxygen levels fall, the activity of HIF-PH enzymes decreases, causing HIF-α subunits to accumulate and dimerize with HIF-β to form functional transcription factors. This process induces adaptive changes in gene expression that either enhance oxygen delivery (e.g., erythropoiesis) or promote survival in a hypoxic environment (Kaelin, 2005; Kaelin and Ratcliffe, 2008; Fong and Takeda, 2008). A fourth oxygen and αKG-dependent enzyme, known as Factor Inhibiting HIF-1α (FIH), hydroxylates HIF-α subunits on an asparagine residue. Hydroxylation by FIH inhibits binding of transcriptional coactivators to HIF-α and thus limits HIF transcriptional activity (Mahon et al., 2001; Lando et al., 2002a; Lando et al., 2002b).

HIF stimulates erythropoiesis via a coordinated response that involves increases in endogenous EPO and enhanced availability of iron for Hb synthesis. HIF directly regulates expression of the EPO gene (Bunn, 2013; Haase, 2010), as well as genes

encoding proteins involved in iron absorption [e.g., divalent metal transporter 1 (DMT1), duodenal cytochrome b (DCYTB)], iron transport (e.g., transferrin), iron mobilization (e.g., ferroportin), and iron recycling (e.g., heme oxygenase-1) (Haase, 2010). Furthermore, activation of the HIF pathway reduces levels of hepcidin, the hormone responsible for iron homeostasis. Elevated hepcidin, which is driven by chronic inflammation, leads to sequestering of iron in enterocytes, macrophages, and hepatocytes, thereby causing functional iron deficiency. Downregulation of hepcidin by activation of the HIF pathway releases iron trapped in cells, thus increasing iron availability for hemoglobin synthesis (Peyssonnaux et al., 2008).

Roxadustat was developed as an orally active inhibitor of the HIF-PH enzymes. In this series of in vitro and in vivo studies, we studied the effects of roxadustat on activation of the HIF pathway, EPO secretion, and stimulation of erythropoiesis in normal rats and monkeys. We also evaluated the ability of roxadustat to correct anemia in two different rodent models. The 5/6th nephrectomy model was used to demonstrate that roxadustat can correct anemia of CKD. The model of anemia of chronic disease (ACD) induced by administration of proteoglycan-polysaccharide (PG-PS) was used to show that roxadustat can reverse anemia associated with inflammation and functional iron deficiency.

Materials and Methods

In Vitro Studies

HIF Hydroxylase Enzyme Assays. Activity of HIF-PH and FIH enzymes was determined based on the capture of $^{14}CO_2$ released by the decarboxylation of [1-^{14}C] αKG (Zhang et al., 1999). Reaction mixtures included Fe(SO$_4$) (Sigma-Aldrich, St. Louis, MO), [1-^{14}C] αKG (Perkin Elmer, Waltham, MA), non-labeled αKG (Sigma-Aldrich, St. Louis, MO), ascorbate (Sigma-Aldrich, St. Louis, MO), peptide-substrate (PHD1,2,3: acetyl-DLDLEMLAPYIPMDDDFQL-amide, FIH: DESGLPQLTSYDCEVNAPIQGSRNLLQGEELLRAL-biotin) (Mimotopes, Mulgrave, Australia), and catalase (cat # C100, Sigma-Aldrich, St. Louis, MO) in 50 mM HEPES buffer (Corning Life Sciences, Tewksbury, MA), pH 7.4. Enzymatic reactions were initiated by addition of full-length recombinant human HIF-PH or FIH enzyme to the reaction mixture (Hirsilä et al., 2005). The reactions were performed in 96-well microtiter plates (100 µl total assay volume) (Thomas Scientific, Santa Clara, CA). $^{14}CO_2$ was captured on a glass fiber–filter paper (Inotech Biosystems International, Brandon, FL) soaked with saturated Ba(OH)$_2$ that was laid on top of the 96-well plate. A microtiter plate–sealer film (Thermal Seal Insulating Glass, Uxbridge, MA) was applied to the filter paper. The plate and filter paper were sandwiched between two custom-made aluminum plates (Advanced Component Manufacturing, Burlingame, CA) and transferred to a 37°C oven for 1–2 hours. After incubation, the filter paper was dried in a 103°C oven for 40–60 minutes. To determine percent turnover, aliquots of the reaction mixture were spotted onto the filter paper, and the filter paper was dried again. The dry filter paper was exposed to a storage phosphor screen for 24–72 hours, and the images

were recorded with a Typhoon FLA 7000 imager (Amersham Biosciences, Piscataway,

NJ). Integrated spot intensities corresponding to control reactions lacking the enzyme

were subtracted from integration results for enzyme-containing reactions, and data were

converted to enzyme-dependent percent-$^{14}CO_2$ release. All enzymatic reactions were

run in duplicate.

To determine the IC_{50} of roxadustat for the HIF-PH and FIH enzymes, a threefold

dilution series of roxadustat (FG-4592; FibroGen, Inc.) was prepared and added to the

reaction mixture [final 1% dimethyl sulfoxide (DMSO), v/v] prior to addition of the

enzyme. The final reagent concentrations were: 1 µM $Fe(SO_4)$, 3 µM [1-^{14}C] αKG, 97

µM non-labeled αKG, 1 mM ascorbate, 50 µM peptide substrate, and ~2 units/µl

catalase. IC_{50} values were determined by non-linear fitting using GraFit version 7.0

(Erithacus Software, UK).

In order to calculate the kinetic parameters for PHD2, turnover velocity was

measured as a function of αKG concentration at varying concentrations of roxadustat.

Non-linear regression analysis was applied to the Michaelis-Menten equation to obtain

apparent V_{max} and K_m using GraFit version 7.0. Double-reciprocal plots of the non-linear

best fits at varying roxadustat concentrations were used to evaluate the mode of

inhibition, while linear fitting of the apparent K_m/V_{max} vs. roxadustat concentration was

used to determine K_i.

Cell Culture. Hep3B cells (cat # HB-8064, American Type Culture Collection,

Manassas, VA) were maintained in Dulbecco's Modified Eagle's Medium (DMEM) (cat #

10-013-CM, Corning Life Sciences, Tewksbury, MA) containing 10% Hyclone fetal

bovine serum (FBS) (cat # SH30071.03, GE Healthcare Life Sciences, Pittsburgh, PA)

under 10% CO_2 conditions at 37°C. Treatment media for Hep3B cells was DMEM containing 0.5% FBS (D0.5). HK-2 cells (cat # CRL-2190, American Type Culture Collection, Manassas, VA) were maintained in Keratinocyte Serum-Free Media supplemented with epidermal growth factor (EGF) and bovine pituitary extract (BPE) (cat # 17005042, Thermo Fisher Scientific, Waltham, MA) under 5% CO_2 conditions at 37°C. Treatment media for HK-2 cells was the same as maintenance media.

Analysis of HIF-1α and HIF-2α Stabilization in Hep3B and HK-2 Cells. Hep3B cells and HK-2 cells were plated into 10-cm dishes at 2×10^6 cells or 8×10^5 cells per dish, respectively. The next day, the cells were treated with 3–30 µM roxadustat or vehicle control (0.15% DMSO) in their respective treatment media. After 3 hours, the cell monolayer was lysed with RIPA lysis buffer (Teknova, Hollister, CA) supplemented with HALT Protease Inhibitors (Thermo Fisher Scientific, Waltham, MA), and whole-cell lysates were collected.

Analysis of HIF-1α Protein Levels in Hep3B Cells Following Removal of Roxadustat. Hep3B cells were plated into 6-cm dishes at 1×10^6 cells per well. The next day, cells were treated with 30 µM roxadustat or vehicle control (0.15% DMSO) in treatment media. After 3 hours, the media was removed, cells were washed, and fresh D0.5 media (without roxadustat or vehicle control) was added. RIPA whole–cell lysates were collected immediately (time "0"), 15, 30, or 60 minutes after removal of roxadustat.

Western Blot Analyses. Protein concentrations of whole-cell lysates were measured using the Pierce BCA Protein Assay Kit (Thermo Fisher Scientific, Waltham, MA). Equal protein was loaded for each sample onto electrophoresis gels. The samples were resolved by SDS-PAGE, transferred to a PVDF membrane (Invitrogen, Carlsbad,

CA), and immunoblotted with HIF-1α (1:1000 dilution, cat # 610959, lot # 23681, BD

Biosciences, San Jose, CA) or HIF-2α (1:1000 dilution, cat # AF2886, lot #

VEA0312021, R&D Systems, Minneapolis, MN) antibodies. The HRP-conjugated

secondary antibodies used were anti-mouse-HRP (1:5000 dilution, cat # 616520,

Invitrogen, Carlsbad, CA) and anti-goat-HRP (1:5000 dilution, cat # 611620, Invitrogen,

Carlsbad, CA), respectively. Bands were visualized using SuperSignal West Pico

Chemiluminescent Substrate (Thermo Fisher Scientific, Waltham, MA) according to the

manufacturer's instructions. For analysis of the tubulin loading control, PVDF

membranes were stripped with Blot Restore Membrane Rejuvenation Kit

(MilliporeSigma, Burlington, MA) prior to immunoblotting with an anti-tubulin antibody

(1:20,000 dilution, cat # T6199, lot # 102M4773V, MilliporeSigma, Burlington, MA) and

an anti-mouse-HRP secondary antibody (1:20,000 dilution, cat # 616520, Invitrogen,

Carlsbad, CA). Scanned Western Blots were quantified using ImageJ software (NIH,

Bethesda, MD). Images were converted to 8-bit images with min-max scales of 0-255.

Selected bands of interest were quantified (mean gray values). Background corrected

values for HIF-α and tubulin were then used to calculate relative levels of HIF-α

normalized to tubulin levels (HIF-α/tubulin). For graphical representation, HIF-α/tubulin

levels were normalized to the 30 μM roxadustat condition for each set of samples. For

quantification of HIF-α levels in the washout experiment, HIF-α/tubulin levels were

normalized to the 30 μM roxadustat, 0 min washout sample.

Roxadustat Induction of Secreted EPO in Hep3B Cells. Hep3B cells were

plated into 96-well plates at 2×10^4 cells per well. The next day, cells were treated with

3–60 μM roxadustat or vehicle control (0.15% DMSO) in treatment media. After 72

hours, conditioned media was collected for EPO analysis by sandwich immunoassay (cat # DEP00, R&D Systems, Minneapolis, MN).

Effects of Inflammatory Cytokines on Secreted EPO in the Presence or Absence of Roxadustat in Hep3B Cells. Hep3B cells were plated into 96-well plates at 5.5 x 10^4 cells per well. The next day, cells were treated with tumor necrosis factor (TNF)α (cat # 210-TA, R&D Systems, Minneapolis, MN), interleukin (IL)-1ß (cat # 201-LB, R&D Systems, Minneapolis, MN), or PBS vehicle control plus either 3–30 μM roxadustat or 0.15% DMSO in treatment media. After 72 hours, conditioned media was collected for EPO analysis by sandwich immunoassay (cat # K15122B, Meso Scale Diagnostics, Rockville, MD).

In Vivo Studies

Procedures in Normal Rats and Monkeys. Pharmacokinetic (PK) parameters for roxadustat were determined in normal male Sprague-Dawley rats ($n = 4$/group) of approximately 8 weeks of age under fasting conditions (Tsukuba Laboratories, Nemoto Science Co., Ibaraki, Japan). All procedures were approved by the Institutional Animal Care and Use Committee of Nemoto Science. Animals were housed individually in metal cages and kept on a 12-hour light-and-dark cycle (lighting: 07:00 AM to 7:00 PM) in an animal holding room with temperature ranging from 20°C to 26°C and humidity ranging from 40% to 70%. Animals weighed 275 to 311 g at the time of drug administration. A dose of 20 mg/kg was administered orally by gavage in a volume of 5 mL/kg (4 mg/mL suspension in 0.5% sodium carboxymethylcellulose and 0.1% Tween 80). The same dose was administered intravenously via the tail vein at a volume of 0.5

mL/kg (40 mg/mL in a saline solution with pH adjusted by NaOH for solubility). Blood samples were collected at times ranging from 0.1 to 48 hours post-dose for determination of plasma roxadustat concentration by liquid chromatography–mass spectrometry (LC-MS).

The time course of EPO secretion in plasma after roxadustat administration was determined in male Sprague Dawley rats (n = 3). Procedures were carried out at FibroGen, Inc. (San Francisco, CA) and approved by the Institutional Animal Care and Use Committee at FibroGen, Inc. Animals were housed individually in standard shoebox-style rat cages. Fluorescent lighting was provided for 12 hours per day between 7:00 AM and 7:00 PM. Temperature was maintained between 20°C and 22°C, and humidity between 35% to 50%. Rodent Laboratory Diet (cat # 5001, PMI Feeds, Inc., St Louis, MO) was withheld overnight before dosing and made available 4 hours post-dose. Tap water was available *ad libitum.* Animals weighed 311–318 g at the time of dosing. A single dose of 30 mg/kg was administered orally in a volume of 5 mL/kg [6 mg/mL suspension in 0.5% sodium carboxymethylcellulose (Spectrum Chemical, Gardena, CA) and 0.1% Polysorbate 80 (Avantor Performance Materials, Radnor, PA)]. Blood samples were collected at regular intervals up to 24 hours post-dose for determination of plasma EPO and roxadustat concentrations. Plasma EPO was measured using the Quantikine Mouse Erythropoietin ELISA kit (R&D Systems, Minneapolis, MN).

The erythropoietic effect of roxadustat was investigated in male Sprague-Dawley rats (Crl: CD) purchased from Charles River Laboratories Japan, Inc. (Hino Breeding Center, Japan). All procedures were carried out in the animal facility at Nihon

Bioresearch, Inc. (Hashima, Japan) following the Basic Guidelines for the Use of Experimental Animals in Institutions under the Jurisdiction of the Japanese Ministry of Health, Labour and Welfare, and the Guidelines for Management and Welfare of Experimental Animals (Nihon Bioresearch, Inc., Japan). The animals were kept on a 12-hour light-and-dark cycle (lighting: 06:00 AM to 6:00 PM) in an animal holding room set at approximately 23°C temperature (range: 21.8°C–24.1°C) and 55% humidity (range: 44.0%–61.1%) with filtered fresh air changes of 12 times per hour. The animals were housed individually in stainless-steel suspended cages and were given free access to solid feed (CRF-1, Oriental Yeast Co., Ltd., Japan) and tap water. Animals weighed 287 to 338 g at study initiation and were assigned to treatment groups such that the mean body weight was similar among groups (n = 8/group). Animals were then treated orally by gavage three times per week for 29 days with vehicle or 6.25, 12.5, 25, or 50 mg/kg roxadustat formulated in 0.5% sodium carboxymethylcellulose (Maruishi Pharmaceuticals, Japan) and 0.1% Tween 80 (Sigma-Aldrich Japan, Japan). The day before administration of the first dose, and before dosing on days 4, 8, 15, and 29 of treatment, about 300 μL of venous blood was collected to measure blood Hb concentration, hematocrit, and reticulocyte number with an XT-2000iV automated hematology analyzer (Sysmex Corporation, Japan). On the last day of treatment, approximately 6 hours after dosing, blood was collected from the abdominal aorta in Venoject® II vacuum heparinized tubes (Terumo Corporation, Japan). After centrifugation at 4°C and 3000 rpm (about 1972 × g) for 15 minutes, plasma was

17

collected to measure EPO concentration with a Mouse/Rat Immunoassay (R&D Systems, Minneapolis, MN).

The erythropoietic effect of roxadustat was also investigated in normal cynomolgus monkeys. All procedures were carried out at Covance Laboratories, Inc. (Vienna, VA) in accordance with the United States Food and Drug Administration Good Laboratory Practice Regulations, Title 21 of the United States Code of Federal Regulations Part 58. Male and female monkeys were housed individually in stainless-steel cages. Animals were offered Certified Primate Diet #2055C (Harlan Teklad) once or twice daily. Water was provided *ad libitum*. Environmental controls for the animal room were set to maintain 18°C to 29°C, a relative humidity of 30% to 70%, a minimum of 10 room-air changes/hour, and a 12-hour light/12-hour dark cycle. The light-and-dark cycle was interrupted on occasion for study-related activities. Twenty-five male and 25 female cynomolgus monkeys weighing 1.9–2.5 kg were used. Blood samples were collected via venipuncture from the femoral vein of non-sedated conscious animals. The animals were randomly assigned to 0, 3, 10, 20, or 30 mg/kg roxadustat, with five animals per sex per group. Animals were orally dosed intermittently (three times per week) for 52 weeks. Blood samples were collected to measure blood Hb concentration and hematocrit with a Siemens Advia 120 twice prior to the first dose and at regular intervals during the 52 weeks of treatment.

Pharmacokinetic parameters for roxadustat were determined in normal male and female cynomolgus monkeys (*n* = 3/group/sex) from a non-naïve PK colony using a complete-crossover design under overnight fasting conditions (Covance, Madison, WI). All procedures were in compliance with the Animal Welfare Act Regulations (9 CFR 3).

Animals were individually housed in stainless-steel cages for the duration of the study. At the time of dosing, body weight ranged from 3.0 to 4.1 kg for males and from 2.9 to 3.4 kg for females. A dose of 30 mg/kg was administered orally by gavage in a volume of 5 mL/kg (6 mg/mL suspension in 0.5% sodium carboxymethylcellulose and 0.1% Tween 80). The same dose was administered intravenously as a slow bolus infusion over approximately 3 minutes via a saphenous vein at 3 mL/kg [10 mg/mL solution in phosphate-buffered saline (PBS) with pH adjusted by NaOH for solubility]. Blood samples were collected at regular intervals for up to 96 hours post-dose for determination of plasma roxadustat concentration by LC-MS.

Rat Model of Anemia Following 5/6 Nephrectomy. Male Sprague Dawley rats (Charles River Laboratories, Hollister, CA) were used to determine the erythropoietic effects of roxadustat in an anemia model of kidney injury induced by 5/6th nephrectomy. All procedures were performed in the animal facility at FibroGen, Inc. (South San Francisco, CA) and were approved by the Institutional Animal Care and Use Committee at FibroGen, Inc. Animals were housed in pairs in standard shoebox-style rat cages. Fluorescent lighting was provided for 12 hours per day between 7:00 AM and 7:00 PM. Temperature was maintained between 20°C and 22°C, and humidity between 40% and 70%, respectively. Rodent Laboratory Diet (cat# 5001, PMI Feeds, Inc., St Louis, MO) and tap water were available *ad libitum.* Animals weighed approximately 300 g at study initiation. Rats were anesthetized with isoflurane (Isoflo, Patterson Veterinary, Dinuba, CA) and a midline abdominal incision was made under sterile conditions followed by blunt dissection of the renal pedicles. Two or three branches of the left renal artery were ligated to infarct 2/3 of the kidney as indicated by a change in kidney color. The right

kidney was then removed, and the abdominal incision was closed. Sham animals underwent the same procedure without left renal artery ligation and right nephrectomy. Animals recovered for 5 weeks until anemia and kidney dysfunction developed, as assessed by complete blood cell count (Cell-Dyn 3700, Abbott Diagnostics, Abbott Park, IL), and serum concentrations of blood urea nitrogen (BUN) and creatinine (Quality Clinical Labs, Mountain View, CA). Nephrectomized animals were then assigned to treatment with vehicle or roxadustat such that all groups had similar mean baseline body weight, hematocrit, Hb, and serum creatinine. Sham animals were similarly assigned to groups. Nephrectomized animals were treated orally by gavage three times per week for one week, followed by twice per week for a second week with vehicle or with 20 or 40 mg/kg roxadustat (FibroGen, Inc.) formulated in 0.5% sodium carboxymethylcellulose (Spectrum Chemical, Gardena, CA) and 0.1% Polysorbate 80 (Avantor Performance Materials, Radnor, PA) ($n = 8–9$ per group). Sham animals were treated with vehicle or 20 mg/kg roxadustat using the same dosing regimen as nephrectomized animals ($n = 8$ per group). Venous blood samples were collected after 7 and 14 days of treatment for blood cell count and serum chemistry analysis.

Rat Model of Anemia of Inflammation. Female Lewis rats (Harlan Laboratories, Indianapolis, IN) were used to determine the erythropoietic effect of roxadustat in a model of anemia of inflammation. All procedures were performed in the animal facility at FibroGen, Inc. (South San Francisco, CA) and were approved by the Institutional Animal Care and Use Committee at FibroGen, Inc. Animals were individually housed in standard shoebox-style rat cages. Fluorescent lighting was provided for 12 hours per day between 7:00 AM and 7:00 PM. Temperature was maintained between 20°C and

22°C, and humidity between 35 and 50%, respectively. Purina Rodent Chow (cat# 5001, PMI Nutrition International, Inc., Brentwood, MO) and tap water were available *ad libitum.* Animals weighed 153 to 176 g at study initiation. Peptidoglycan-polysaccharide polymers (PG-PS) from Streptococcus pyogenes (PG-PS 10S; Lee Laboratories, Grayson, GA) were administered intraperitoneally in physiological saline at 15 mg/kg of rhamnose to induce anemia. Sham (unchallenged) animals were administered physiological saline. Four weeks after injection of PG-PS, complete blood cell count was determined (Cell-Dyn 3700; Abbott Diagnostics, Abbott Park, IL) and animals were assigned to treatment groups such that all PG-PS-challenged groups had similar mean baseline hematocrits. PG-PS-challenged animals with hematocrit above 35% were considered non-responsive and not used in the study. Unchallenged animals were similarly assigned to groups. Animals were then treated orally by gavage three times per week with 30 mg/kg roxadustat formulated in 0.5% sodium carboxymethylcellulose (Spectrum Chemical, Gardena, CA) and 0.1% Polysorbate 80 (Avantor Performance Materials, Radnor, PA) (n = 8 PG-PS-challenged; n = 4 unchallenged) or vehicle (n = 8 PG-PS-challenged; n = 4 unchallenged). Animals were also treated intravenously with darbepoetin alfa (Aranesp, Amgen, Thousand Oaks, CA) every other week at 30 μg/kg (n = 7 PG-PS-challenged; n = 4 unchallenged) or sodium ferric gluconate complex (Ferrlecit; Watson Pharma) once per week at 1.5 mg/kg (n = 7 PG-PS-challenged; n = 4 unchallenged). Venous blood samples were collected after 14 and 28 days of treatment for blood cell count, and after 28 days for serum iron and cytokine measurements. A multiplex cytokine panel was run for IL-1α, IL-1ß, IL-4, TNFα, granulocyte-macrophage colony-stimulating factor (GM-CSF), IL-6, and macrophage inflammatory protein (MIP)-

3α on serum samples. After the last blood sample, animals were euthanized, and their front paws were harvested and weighed to quantify inflammation. Liver and duodenum were harvested and processed for quantitative real-time PCR (qRT-PCR).

Gene Expression Analysis. Liver and duodenum tissue samples were stored in Ambion RNAlater solution (Thermo Fisher Scientific, Waltham, MA). RNA was isolated by homogenization in Trizol (Invitrogen, Carlsbad, CA) and further purified on RNeasy96 columns (Qiagen, Germany). Complementary DNA was prepared from total RNA using Omniscript reverse transcriptase (Qiagen, Germany) and random hexamer primers. qRT-PCR was performed in a Prism 7000 (Applied Biosystems, Foster City, CA) instrument using TaqMan Universal PCR Master Mix (Applied Biosystems, Foster City, Ca) and TaqMan Assays-on-Demand (Applied Biosystems, Foster City, CA) assays. Quantitative PCR data for *Dcytb* (duodenal cytochrome b gene), *Dmt1* (a.k.a. *Slc11a2*, iron transporter DMT1 gene), and *Hamp* (hepcidin gene) were normalized to 18S ribosomal RNA expression.

Statistics. All in vitro data is presented as mean ± standard deviation (SD). Data from cell-based studies was analyzed using analysis of variance (ANOVA) followed by Dunnett's multiple comparison test. All in vivo data is presented as mean ± standard error of the mean (SEM). Data from in vivo studies was analyzed using ANOVA followed by a multiple comparison procedure at each time point (Student-Newman-Keuls Method). Steel's test was performed to analyze in vivo EPO results. When values of EPO were below the lower limit of quantification (47.0 pg/mL), the lower limit of

quantification was used for statistical analysis. A P value less than 0.05 was considered

statistically significant for all tests.

Results

Roxadustat is an Inhibitor of HIF-PH Enzymes that Reversibly Stabilizes HIF-1α and HIF-2α. Roxadustat (FG-4592) was selected from a series of 4-hydroxyisoquinoline glycinamides that were designed to inhibit HIF-PH enzymes by competing with the substrate αKG. The ability of roxadustat to inhibit recombinant full-length human HIF-PH enzymes was measured using an enzyme assay based on the decarboxylation of ^{14}C-labeled αKG and the production of $^{14}CO_2$ (Zhang et al., 1999). In the presence of 100 μM αKG, 1 μM Fe^{2+}, and 1 mM ascorbate, roxadustat IC_{50} values of 1.04 ± 0.46 μM, 1.74 ± 0.73 μM, and 0.36 ± 0.12 μM were obtained for PHD1, PHD2, and PHD3, respectively (mean ± SD, n = 9–10). The dependence of PHD2 activity on αKG concentration at several concentrations of roxadustat yielded invariable V_{max} and variable K_m, indicating competitive inhibition kinetics with respect to αKG, and a K_i value for roxadustat of 20 ± 3 nM (Supplementary Fig. 1; Supplementary Table 1). The selectivity of roxadustat for the HIF-PH enzymes over FIH was determined by measuring roxadustat's ability to inhibit recombinant full-length human FIH under the same assay conditions as those used for the HIF-PH enzymes. Under those conditions, the FIH IC_{50} for roxadustat was >150 μM.

The ability of roxadustat to stabilize HIF-α was explored in two human cell lines, Hep3B hepatoma cells and HK-2 renal proximal tubule cells. In both lines, incubation with roxadustat for 3 hours dose-dependently increased HIF-1α and HIF-2α protein levels (Fig. 1A & Supplementary Fig. 2A and 2B). The reversibility of HIF-α stabilization by roxadustat was investigated by performing washout studies in Hep3B cells. Compared to DMSO-treated cells, Hep3B cells treated with 30 μM roxadustat for 3

hours and then harvested immediately exhibited an accumulation of HIF-1α protein. In cells treated with roxadustat for 3 hours and harvested at 15, 30, or 60 minutes after washout of the drug, HIF-1α levels rapidly decreased back to basal levels (Fig. 1B & Supplementary Fig. 2C). A reduction in HIF-1α protein was observed 15 minutes after washout, and by 60 minutes, HIF-1α was no longer detectable.

Roxadustat Stimulates EPO Production in Cells and Overcomes the Suppressive Effects of Inflammatory Cytokines. The ability of roxadustat to increase production of EPO, a well-known HIF target gene, was investigated in Hep3B cells. Exposure of Hep3B cells to roxadustat dose-dependently increased EPO protein secreted into the culture supernatant (Fig. 2A). EPO production is suppressed by pro-inflammatory cytokines, such as TNFα and IL-1ß (Jelkmann et al., 1994; La Ferla et al., 2002). We found that both of these cytokines dose-dependently decreased EPO protein secreted by Hep3B cells (Fig. 2B and 2C). We explored whether roxadustat could overcome this suppressed EPO production. Hep3B cells were treated with increasing concentrations of roxadustat in the presence of either 0.125 ng/mL TNFα or 0.125 ng/mL IL-1ß, concentrations that robustly suppress EPO production (Fig. 2B and 2C). Even in the presence of these pro-inflammatory cytokines, roxadustat dose-dependently increased EPO production from Hep3B cells (Fig. 2D and 2E).

Pharmacokinetics of Roxadustat and Time Course of EPO Secretion in Rats and Monkeys. When dosed intravenously at 20 mg/kg in rats and 30 mg/kg in monkeys, roxadustat showed low systemic clearances in rats and monkeys that were much lower than hepatic blood flow, and Vdss (134–178 mL/kg) that were larger than plasma volume but less than total body water (Table 1). Oral bioavailability was high in

both species (70%–100%). Plasma roxadustat peaked 2 hours following a 30 mg/kg oral dose in rats, whereas maximum plasma EPO concentration was achieved 8–12 hours post-dose (Fig. 3). Twenty-four hours after dosing, roxadustat plasma concentrations were at low levels (less than 5% of Cmax), and EPO levels were close to baseline levels.

Roxadustat Increases Circulating EPO Concentration and Erythropoiesis in Normal Rats. The in vivo erythropoietic effect of roxadustat was evaluated in normal rats at doses ranging from 6.25 to 50 mg/kg administered 3 times per week for 29 days. Blood Hb concentration and hematocrit gradually increased over time in a dose-dependent manner. The 12.5 mg/kg dose induced a modest 0.9 g/dL rise in Hb over vehicle by Day 29, whereas the high dose (50 mg/kg) increased Hb by 5.8 g/dL compared to vehicle (Fig. 4A). Reticulocytes also increased in a dose-dependent manner, and maximum responses were seen on Days 4 and 8 of treatment in the 25 and 50 mg/kg groups, respectively. Reticulocytes gradually returned to vehicle levels in the 25 mg/kg group, but they remained elevated compared to the vehicle group after 29 days of treatment with 50 mg/kg (Fig. 4C). Plasma EPO concentrations after 29 days of treatment with 12.5, 25, and 50 mg/kg roxadustat were significantly higher than in the vehicle group. Plasma EPO was more than 7 times higher in the 12.5 mg/kg group than in the vehicle group, whereas it was more than 300 times higher in the 50 mg/kg group than in the vehicle group. EPO concentration was below the lower limit of quantification in all vehicle-treated animals and in 7 of 8 animals in the 6.25 mg/kg group (Fig. 4D).

Roxadustat Increases Erythropoiesis in Normal Cynomolgus Monkeys. In a 52-week intermittent-dosing study in male and female cynomolgus monkeys, Hb was

measured prior to the first dose and at regular intervals during the dosing period.

Monkeys administered ≥ 20 mg/kg roxadustat three times per week exhibited increased erythropoiesis, with significant increases in Hb apparent following 2 weeks of dosing (Fig. 5A). The transient decrease in Hb observed in all groups during the first week of treatment was due to multiple bleeds performed in the days preceding the Hb measurement to assess drug exposure. Red blood cell count was also significantly elevated at doses ≥ 20 mg/kg (Fig. 5B).

Roxadustat Corrects Anemia in Rats after 5/6th Nephrectomy. The erythropoietic activity of roxadustat was determined in a rat model of anemia of CKD induced by 5/6th nephrectomy. Nephrectomy resulted in anemia, as shown by lower Hb (Fig. 6A), hematocrit (Fig. 6B), and red blood cell count (Fig. 6C) than sham surgery. Nephrectomized animals also had higher levels of BUN and serum creatinine than sham animals, indicating progressive kidney failure (Supplementary Fig. 3). After 2 weeks of intermittent dosing, treatment with 20 and 40 mg/kg roxadustat significantly increased and normalized Hb (Fig. 6A), hematocrit (Fig. 6B), and red blood cell count (Fig. 6C) in nephrectomized animals compared to the vehicle control group. BUN and serum creatinine values were not affected by treatment with roxadustat (Supplementary Fig. 3).

Roxadustat Corrects Anemia of Inflammation in a Rat Model of ACD. The efficacy of roxadustat in correcting anemia was investigated in a rat model of PG-PS-induced chronic inflammation. Hb was below 10 g/dL in all PG-PS-challenged groups before treatment initiation, indicating severe anemia (Fig. 7A). Mean corpuscular

volume (MCV) and mean corpuscular Hb concentration (MCHC) were also reduced in anemic animals, indicating microcytosis and hypochromia, respectively.

Treating anemic PG-PS-challenged animals with 30 mg/kg roxadustat three times per week for 4 weeks increased their Hb to levels similar to non-challenged animals administered vehicle (Fig. 7A). Roxadustat also improved the microcytosis (increased MCV, Fig. 7B) and hypochromia (increased MCHC, Fig. 7C) observed in the PG-PS-challenged groups. In contrast, darbepoetin and intravenous (IV) iron had no effect on Hb, MCV, or MCHC in anemic PG-PS-challenged animals.

In non-challenged animals, treatment with either roxadustat or darbepoetin produced a robust erythropoietic response. After 2 weeks of treatment with roxadustat or darbepoetin, Hb was significantly higher than in the vehicle group, and the erythropoietic response was maintained at 4 weeks with both treatments (Fig. 7A). IV iron had no effect on erythropoiesis in non-challenged animals (Fig. 7A).

Roxadustat Does Not Affect the Inflammatory Response in a Rat Model of ACD. Animals challenged with PG-PS developed an inflammatory response. These animals exhibited increased circulating white blood cells (WBC), including monocytes (Supplementary Fig. 4A and 4B), neutrophils, lymphocytes, and eosinophils (data not shown). These animals also displayed increased paw weight, suggesting that they developed arthritis (Supplementary Fig. 4C). Treatment with roxadustat significantly decreased the monocyte count (Supplementary Fig. 4B) but did not affect other WBC types (data not shown). Darbepoetin and IV iron had no effect on the WBC response in PG-PS-challenged animals. Paw weight was not significantly affected by any of the treatment regimens (Supplementary Fig. 4C).

A multiplex cytokine panel was run on serum samples taken after 4 weeks of treatment. Values for IL-1ß, IL-4, TNFα, and GM-CSF were below the levels of quantitation in most samples (data not shown). IL-6 was primarily measurable in samples from PG-PS-challenged animals, and MIP-3a was measurable in nearly all samples. IL-6 and MIP-3a levels were not significantly reduced after treatment with roxadustat in PG-PS-challenged animals, although the data suggest a trending decline. Serum IL-6 was increased in the darbepoetin group and IV iron had no effect on serum cytokines (Supplementary Fig. 4D).

Roxadustat Improves Iron Metabolism in a Rat Model of ACD. At the end of the ACD study, PG-PS-challenged animals treated with vehicle had lower serum iron (Fig. 8A) and transferrin saturation (Fig. 8B), as well as higher total iron–binding capacity (a measure of serum transferrin level, Fig. 8C), than vehicle-treated animals not challenged with PG-PS. In PG-PS-challenged animals, roxadustat significantly improved serum iron levels (Fig. 8A) and transferrin saturation (Fig. 8B) without affecting total iron–binding capacity (Fig. 8C) compared to vehicle. Neither darbepoetin nor IV iron had any significant effect on iron parameters compared to vehicle.

qPCR was used to quantify hepatic gene expression of *Hamp* (which encodes the protein hepcidin, a key regulator of iron metabolism and mediator of anemia of inflammation), and duodenal gene expression of *Dcytb* (a ferric reductase enzyme required for intestinal absorption of iron) and *Dmt1* (a transporter of iron through apical membranes). Roxadustat reduced expression of hepatic *Hamp* (Fig. 9A) in PG-PS-challenged animals and increased expression of *DcytB* (Fig. 9B) and *Dmt1* (Fig. 9C) in

the duodenum of PG-PS-challenged animals. Darbepoetin and IV iron had no significant

effect on *Hamp*, *DcytB*, or *Dmt1* expression.

Discussion

Several HIF-PH inhibitors are being evaluated in clinical trials as novel therapeutics to treat anemia of CKD (Gupta and Wish, 2017; Del Vecchio and Locatelli, 2018). In December 2018, roxadustat became the first HIF-PH inhibitor to receive marketing approval in any country when China's National Medical Products Administration approved it for the treatment of anemia of CKD in dialysis-dependent patients (Dhillon, 2019). We present here the pharmacological profile of roxadustat, an inhibitor of HIF-PH enzymes with similar potency for all three isoforms (PHD1, PHD2, and PHD3). The IC_{50} values for PHD1–3 were between 0.36 and 1.74 µM under our assay conditions. Roxadustat displays competitive inhibition kinetics with respect to αKG, and therefore the αKG concentration in the enzyme reaction will significantly influence the calculated IC_{50}. We chose 100 µM αKG for our enzyme assays based on published reports of intracellular αKG concentrations (Nagai et al., 1998; MacKenzie et al., 2007). Assays carried out with lower αKG concentrations would be expected to yield lower IC_{50} values (Yeh et al., 2017).

In cells, both HIF-1α and HIF-2α were stabilized by roxadustat at concentrations as low as 3 µM, consistent with the observation that roxadustat inhibits all three HIF-PH enzymes. HIF-α protein levels rapidly declined following washout of roxadustat from cell cultures, indicating that HIF-PH inhibition is reversible, and that once the drug is removed, hydroxylation and degradation of HIF-α subunits quickly resumes.

Although HIF-1 was initially identified as the transcription factor responsible for the hypoxic induction of EPO (Semenza & Wang, 1992; Wang & Semenza, 1995; Wang et al., 1995), studies in mice and analysis of genetic mutations in patients with inherited

polycythemia have since revealed that HIF-2 is the main regulator of EPO production (Rankin et al., 2007; Percy, 2008; Kapitsinou et al., 2010). In our studies, stabilization of HIF-2α in Hep3B cells by roxadustat was accompanied by a dose-dependent increase in EPO production. HIF-2 also modulates intestinal iron uptake by regulating expression of DMT1 and DCYTB (Mastrogiannaki et al., 2009; Shah et al., 2009; Mastrogiannaki et al., 2012). However, other HIF-regulated genes involved in iron metabolism and erythropoiesis appear to depend more on HIF-1 than on HIF-2 (Rolfs et al., 1997; Tacchini et al., 1999; Zhang et al., 2011), suggesting that stabilization of both HIF-2α and HIF-1α is desirable for an optimal erythropoietic response.

Roxadustat exhibits considerable selectivity for the HIF-PH enzymes over the asparaginyl hydroxylase FIH, with an $IC_{50} > 150$ μM for FIH compared with 0.36–1.74 μM for PHD1–3. Hydroxylation of HIF-α by FIH blocks the interaction between HIF-α and the p300/CBP family of co-activators, and as a result limits the transcriptional activity of HIF (Mahon et al., 2001; Lando et al., 2002a; Lando et al., 2002b). Certain HIF target genes are sensitive to FIH hydroxylation of HIF-α and are not optimally induced unless both HIF-PH enzymes and FIH are inhibited. Conversely, a subset of HIF target genes are relatively insensitive to FIH activity and can be induced by HIF-PH inhibition alone (Dayan et al., 2006; Chan et al., 2016). Because roxadustat inhibits HIF-PH enzymes but not FIH, the compound likely elicits a more limited HIF transcriptional response than conditions in which both HIF-PH and FIH are suppressed, such as severe hypoxia (Chan et al., 2016). The proangiogenic gene vascular endothelial growth factor (VEGF) is an example of an FIH-inhibited HIF target gene (Dayan et al., 2006). No increase in the risk of neoplasia was observed in nonclinical carcinogenicity

studies and in VEGF-dependent tumor models. (Beck et al., 2017; Seeley at al., 2017). Furthermore, changes in systemic VEGF levels with HIF-PH inhibitors such as roxadustat have not been reported in phase 2a studies (Locatelli et al., 2017).

Pharmacokinetic studies showed that roxadustat exhibited low clearance, high oral bioavailability, and half-lives of approximately 4 hours in rats and 11 hours in monkeys. Roxadustat administered orally three times per week to healthy rats for 29 days increased circulating EPO levels, blood Hb, hematocrit, and reticulocytes in a dose-dependent manner. The increase in reticulocyte count was maximal 4–8 days after initiation of treatment. Blood Hb and hematocrit rose steadily over the 29 days of dosing. EPO plasma concentration peaked 6–10 hours after peak drug plasma level, consistent with upregulation of gene expression and protein synthesis. Plasma EPO levels remained elevated for a few hours and declined to baseline 24 hours after dosing, showing that transient stimulation of EPO production by intermittent dosing is sufficient for significant erythropoiesis to occur. Roxadustat was equally effective when administered intermittently to cynomolgus monkeys.

We studied the effect of roxadustat on anemia associated with chronic renal failure using 5/6th-nephrectomized rats. This model is commonly used to study CKD and its complications, including anemia (Garrido et al., 2015; de Mik et al., 2013; Ribeiro et al., 2016). Roxadustat, administered for 2 weeks (20 and 40 mg/kg) in nephrectomized rats, dose-dependently normalized Hb, hematocrit, and red blood cell count compared to control rats. In the clinical setting, roxadustat increased blood Hb in anemic CKD patients (Besarab et al., 2015; Besarab et al., 2016; Provenzano et al., 2016a; Chen et al., 2019a; Chen et al., 2019b).

Inflammatory cytokines such as TNFα and IL-1β suppress EPO production in cell culture and in isolated-perfused rat kidneys (La Ferla et al., 2002; Jelkmann et al., 1994). This suppression may contribute to the pathophysiology of anemia of CKD. In Hep3B cells, we observed a decrease in EPO production following exposure to either TNFα or IL-1β. Despite the suppression of basal EPO production by these inflammatory cytokines, roxadustat induced a dose-dependent increase in EPO in the presence of TNFα and IL-1β.

The erythropoietic activity of roxadustat in the context of inflammation and impaired iron metabolism, was evaluated in a rat model of anemia of inflammation induced by PG-PS. Four weeks of oral treatment with 30 mg/kg roxadustat three times per week corrected PG-PS-induced anemia in rats. Roxadustat also improved iron use, as shown by amelioration of microcytosis and hypochromia in PG-PS-injected animals. Serum iron and transferrin saturation were also mildly but significantly elevated indicating improved mobilization of iron stores to support erythropoiesis. Hepcidin is a key regulator of iron metabolism and a mediator of anemia of inflammation (Deicher and Hörl, 2004). Roxadustat significantly decreased *Hamp* mRNA (hepcidin) expression in liver, which may explain the improved iron status and hematology observed in PG-PS-injected animals treated with roxadustat. Intestinal iron absorption by duodenal enterocytes requires DCYTB to reduce ferric iron to ferrous iron (Fe^{2+}) and DMT1 to transport Fe^{2+} through apical membranes. Roxadustat significantly increased *DcytB* and *Dmt1* mRNA in the duodenum of PG-PS-injected animals pointing to a potential mechanism by which iron availability is improved, consistent with HIF activation (Haase, 2010; Anderson et al., 2011). Roxadustat had little effect on inflammation in this model,

indicating that the anti-anemic properties of roxadustat were not due to inhibition of the inflammatory response induced by PG-PS.

Conversely, the EPO analogue darbepoetin administered every other week increased erythropoiesis in normal animals over a 4-week period but did not correct anemia of inflammation in the PG-PS model. The lack of efficacy of EPO analogues in this model was previously reported with recombinant human EPO (Barrett et al., 2011; Barrett et al., 2015). These results indicate that darbepoetin is not as efficacious in stimulating erythropoiesis in the context of inflammation as in normal animals. Darbepoetin, unlike roxadustat, had no significant effect on iron metabolism, including serum iron, transferrin saturation, and mRNA expression of *Hamp*, *DcytB*, or *Dmt1*. These results may explain darbepoetin's lack of efficacy in this anemia model of functional iron deficiency (Sartor et al., 1989). Finally, the lack of effect of IV iron therapy in this study agrees with the functional iron deficiency seen in the PG-PS model. Iron supplementation alone could not overcome iron sequestration in these animals.

In clinical trials, roxadustat administered intermittently corrected anemia in CKD patients independently of iron or inflammatory status (Besarab et al., 2016; Provenzano et al., 2016a). It also reduced serum hepcidin levels and increased serum transferrin concentrations, improving iron delivery to bone marrow (Besarab et al., 2016; Chen et al., 2019b). Because roxadustat improved iron status, IV-iron supplementation was not required for efficacy in contrast to treatment with ESAs (Besarab et al., 2015; Provenzano et al., 2016a). Inflammation in CKD patients is associated with hyporesponsiveness to ESAs, and the link between hyporesponsiveness and

inflammation may be functional iron deficiency due to elevated hepcidin (MacDougall and Cooper, 2005; Adamson, 2009; Yilmaz et al., 2011). The coordinated erythropoiesis resulting from both increased EPO secretion and improved iron status explains the efficacy of roxadustat against anemia in the context of inflammation. It also accounts for the correction of anemia by roxadustat with relatively low concentrations of circulating endogenous EPO compared to the supraphysiologic serum EPO levels achieved after treatment with ESAs (Besarab et al., 2015; Provenzano et al., 2016b).

In conclusion, roxadustat inhibits all three HIF-PH isoforms, stabilizes HIF-1α and HIF-2α, and dose-dependently increases EPO production in vitro, both in the absence and presence of inflammatory cytokines. Roxadustat exhibits erythropoietic activity in normal rats and monkeys, and corrects anemia in rat models of CKD and of chronic inflammation with impaired iron metabolism. The coordinated erythropoietic response induced by roxadustat involving both increased EPO secretion and mobilization of iron stores makes this drug a promising treatment for anemia of CKD and anemia associated with functional iron deficiency.

Acknowledgements

Authorship Contributions

Participated in research design: Signore, Walkinshaw, Seeley, Brenner, Wang, Guo, Flippin, Chow, Langsetmo, Guenzler, Liu, Klaus, Neff, Lin, del Balzo

Conducted experiments: Wang, Guo, Arend, Chow, Gervasi, Kjaergaard, Langsetmo

Contributed new reagents or analytic tools: N/A

Performed data analysis: Signore, Walkinshaw, Seeley, Brenner, Wang, Guo, Chow, Gervasi, Langsetmo, del Balzo

Wrote or contributed to the writing of the manuscript: Signore, del Balzo, Walkinshaw

References

Adamson JW (2009) Hyporesponsiveness to erythropoiesis stimulating agents in chronic kidney disease: the many faces of inflammation. *Adv Chronic Kidney Dis* **16:** 76-82.

Anderson ER, Xue X, and Shah YM (2011) Intestinal hypoxia-inducible factor-2α (HIF-2α) is critical for efficient erythropoiesis. *J Biol Chem* **286:** 19533-19540.

Babitt JL and Lin HY (2012) Mechanisms of anemia in CKD. *J Am Soc Nephrol* **23:** 1631-1634.

Barrett TD, Palomino HL, Brondstetter TI, Kanelakis KC, Wu X, Haug PV, Yan W, Young A, Hua H, Hart JC, Tran D-T, Venkatesan H, Rosen MD, Peltier HM, Sepassi K, Rizzolio MC, Bembenek SD, Mirzadegan T, Rabinowitz MH, and Shankley NP (2011) Pharmacological characterization of 1-(5-Chloro-6-(trifluoromethoxy)-1*H*-benzoimidazol-2-yl)-1*H*-pyrazole-4-carboxylic acid (JNJ-42041935), a potent and selective hypoxia-inducible factor prolyl hydroxylase inhibitor. *Mol Pharmacol* **79:** 910-920.

Barrett TD, Palomino HL, Brondstetter TI, Kanelakis KC, Wu X, Yan W, Merton KP, Schoetens F, Ma JY, Skaptason J, Gao J, Tran D-T, Venkatesan H, Rosen MD, Shankley NP, and Rabinowitz MH (2015) Prolyl hydroxylase inhibition corrects functional iron deficiency and inflammation-induced anaemia in rats. *Br J Pharmacol* **172:** 4078-4088.

Beck J, Henschel C, Chou J, Lin A, del Balzo U (2017) Evaluation of the carcinogenic potential of roxadustat (FG-4592), a small molecule inhibitor of hypoxia-inducible factor prolyl hydroxylase in CD-1 mice and Sprague Dawley rats. *Int J Toxicol* **36**: 427-439.

Besarab A, Provenzano R, Hertel J, Zabaneh R, Klaus SJ, Lee T, Leong R, Hemmerich S, Yu K-HP, and Neff TB (2015) Randomized placebo-controlled dose-ranging and pharmacodynamics study of roxadustat (FG-4592) to treat anemia in nondialysis-dependent chronic kidney disease (NDD-CKD) patients. *Nephrol Dial Transplant* **30:** 1665-1673.

Besarab A, Chernyavskaya E, Motylev I, Shutov E, Kumbar LM, Gurevich K, Chan DTM, Leong R, Poole L, Zhong M, Saikali KG, Franco M, Hemmerich S, Yu K-HP, and Neff TB (2016) Roxadustat (FG-4592): correction of anemia in incident dialysis patients. *J Am Soc Nephrol* **27:** 1225-1233.

Biggar P and Kim G-H (2017) Treatment of renal anemia: erythropoiesis stimulating agents and beyond. *Kidney Res Clin Pract* **36:** 209-223.

Bunn HF (2013) Erythropoietin. *Cold Spring Harb Perspect Med* doi: 10.1101/cshperspect.a011619.

Chan MC, Ilott NE, Schödel J, Sims D, Tumber A, Lippl K, Mole DR, Pugh CW, Ratcliffe PJ, Ponting CP, and Schofield CJ (2016) Tuning the transcriptional response to hypoxia by inhibiting hypoxia-inducible factor (HIF) prolyl and asparaginyl hydroxylases. *J Biol Chem* **291:** 20661-20673.

Chen N, Hao C, Peng X, Lin H, Yin A, Hao L, Tao Y, Liang X, Liu Z, Xing C, Chen J, Luo L, Zuo L, Liao Y, Liu B-C, Leong R, Wang C, Liu C, Neff T, Szczech L, Yu K-HP. (2019a) Roxadustat for anemia in patients with kidney disease not receiving dialysis. *N Engl J Med* **381**: 1001-1010.

Chen N, Hao C, Liu B-C, Lin H, Wang C, Xing C, Liang X, Jiang G, Liu Z, Li X, Zuo L, Luo L, Wang J, Zhao M-H, Liu Z, Cai G-Y, Hao L, Leong R, Wang C, Liu C, Neff T, Szczech L, Yu K-HP (2019b) Roxadustat treatment for anemia in patients undergoing long-term dialysis. *N Engl J Med* **381**: 1011-1022.

Dayan F, Roux D, Brahimi-Horn MC, Pouyssegur J, and Mazure NM (2006) The oxygen sensor factor-inhibiting hypoxia-inducible factor-1 controls expression of distinct genes through the bifunctional transcriptional character of hypoxia-inducible factor-1alpha. *Cancer Res* **66:** 3688-3698.

de Mik SML, Hoogduijn MJ, de Bruin RW, and Dor FJMF (2013) Pathophysiology and treatment of focal segmental glomerulosclerosis: the role of animal models. *BMC Nephrol* **14:** 74.

Deicher R and Hörl WH (2004) Hepcidin: a molecular link between inflammation and anaemia. *Nephrol Dial Transplant* **19:** 521-524.

Del Vecchio L and Locatelli F (2018) Investigational hypoxia-inducible factor prolyl hydroxylase inhibitors (HIF-PHI) for the treatment of anemia associated with chronic kidney disease. *Expert Opin Investig Drugs* **27:** 613-621.

Dhillon S (2019) Roxadustat: first global approval. *Drugs* **79:** 563-572.

Finkelstein FO, Story K, Firanek C, Mendelssohn D, Barre P, Takano T, Soroka S, and
Mujais S (2009) Health-related quality of life and hemoglobin levels in chronic
kidney disease patients. *Clin J Am Soc Nephrol* **4:** 33-38.

Fong G-H and Takeda K (2008) Role and regulation of prolyl hydroxylase domain
proteins. *Cell Death Differ* **15:** 635-641.

Garrido P, Ribeiro S, Fernandes J, Vala H, Bronze-da-Rocha E, Rocha-Pereira P, Belo
L, Costa E, Santos-Silva A, and Reis F (2015) Iron-hepcidin dysmetabolism,
anemia and renal hypoxia, inflammation and fibrosis in the remnant kidney rat
model. *PLoS ONE* doi: 10.1371/journal.pone.0124048.

Gupta N and Wish JB (2017) Hypoxia-inducible factor prolyl hydroxylase inhibitors: a
potential new treatment for anemia in patients with CKD. *Am J Kidney Dis* **69:**
815-826.

Haase VH (2010) Hypoxic regulation of erythropoiesis and iron metabolism. *Am J
Physiol Renal Physiol* **299:** F1-F13.

Hirsilä M, Koivunen P, Xu L, Seeley T, Kivirikko KI, and Myllyharju J (2005) Effect of
desferrioxamine and metals on the hydroxylases in the oxygen sensing pathway.
FASEB J **19:** 1308-1310.

Jelkmann WE, Fandrey J, Frede S, and Pagel H (1994) Inhibition of erythropoietin

production by cytokines. Implications for the anemia involved in inflammatory

states. *Ann N Y Acad Sci* **718:** 300-309.

Kaelin WG Jr and Ratcliffe PJ (2008) Oxygen sensing by metazoans: the central role of

the HIF hydroxylase pathway. *Mol Cell* **30:** 393-402.

Kaelin WG (2005) Proline hydroxylation and gene expression. *Annu Rev Biochem* **74:**

115–128.

Kapitsinou PP, Liu Q, Unger TL, Rha J, Davidoff O, Keith B, Epstein JA, Moores SL,

Erickson-Miller CL, and Haase VH (2010) Hepatic HIF-2 regulates erythropoietic

responses to hypoxia in renal anemia. *Blood* **116:** 3039-3048.

Kassebaum NJ, Jasrasaria R, Naghavi M, Wulf SK, Johns N, Lozano R, Regan M,

Weatherall D, Chou DP, Eisele TP, Flaxman SR, Pullan RL, Brooker SJ, and

Murray CJL (2014) A systematic analysis of global anemia burden from 1990 to

2010. *Blood* **123:** 615-624.

La Ferla K, Reimann C, Jelkmann W, and Hellwig-Bürgel T (2002) Inhibition of

erythropoietin gene expression signaling involves the transcription factors GATA-

2 and NF-kappaB. *FASEB J* **16:** 1811-1813.

Lando D, Peet DJ, Gorman JJ, Whelan DA, Whitelaw ML, and Bruick RK (2002a) FIH-1

is an asparaginyl hydroxylase enzyme that regulates the transcriptional activity of

hypoxia-inducible factor. *Genes Dev* **16:** 1466-1471.

Lando D, Peet DJ, Whelan DA, Gorman JJ, and Whitelaw ML (2002b) Asparagine hydroxylation of the HIF transactivation domain a hypoxic switch. *Science* **295:** 858-861.

Locatelli F, Fishbane S, Block GA, and Macdougall IC (2017) Targeting hypoxia-inducible factors for the treatment of anemia in chronic kidney disease patients. *Am J Nephrol* **45:** 187-199.

Macdougall IC and Cooper AC (2005) Hyporesponsiveness to erythropoietic therapy due to chronic inflammation. *Eur J Clin Invest* **35:** 32-35.

MacKenzie ED, Selak MA, Tennant DA, Payne LJ, Crosby S, Frederiksen CM, Watson DG, and Gottlieb E (2007) Cell-permeating alpha-ketoglutarate derivatives alleviate pseudohypoxia in succinate dehydrogenase-deficient cells. *Mol Cell Biol* **27:** 3282-3289.

Mahon PC, Hirota K, and Semenza GL (2001) FIH-1: a novel protein that interacts with HIF-1alpha and VHL to mediate repression of HIF-1 transcriptional activity. *Genes Dev* **15:** 2675-2686.

Mastrogiannaki M, Matak P, Keith B, Simon MC, Vaulont S, and Peyssonnaux C (2009) HIF-2alpha, but not HIF-1alpha, promotes iron absorption in mice. *J Clin Invest* **119:** 1159–1166.

Mastrogiannaki M, Matak P, Delga S, Deschemin J-C, Vaulont S, and Peyssonnaux C
(2012) Deletion of HIF-2α in the enterocytes decreases the severity of tissue iron
loading in hepcidin knockout mice. *Blood* **119:** 587–590.

Myllyharju J (2013) Prolyl 4-hydroxylases, master regulators of the hypoxia response.
Acta Physiol (Oxf) **208:** 148-165.

Naets JP (1963) Relation between erythropoietin plasma level and oxygen
requirements. *Proc Soc Exp Biol Med* **112:** 832-836.

Nagai J, Yano I, Hashimoto Y, Takano M, and Inui K (1998) Efflux of intracellular alpha-
ketoglutarate via p-aminohippurate/dicarboxylate exchange in OK kidney
epithelial cells. *J Pharmacol Exp Ther* **285:** 422-427.

Percy MJ (2008) Familial erythrocytosis arising from a gain-of-function mutation in the
HIF2A gene of the oxygen sensing pathway. *Ulster Med J* **77:** 86-88.

Peyssonnaux C, Nizet V, and Johnson RS (2008) Role of hypoxia inducible factors in
iron metabolism. *Cell Cycle* **7:** 28-32.

Pfeffer MA, Burdmann EA, Chen C-Y, Cooper ME, de Zeeuw D, Eckardt K-U, Feyzi JM,
Ivanovich P, Kewalramani R, Levey AS, Lewis EF, McGill JB, McMurray JJ,
Parfrey P, Parving H-H, Remuzzi G, Singh AK, Solomon SD, Toto R, and TREAT
Investigators (2009) A trial of darbepoetin alfa in type 2 diabetes and chronic
kidney disease. *N Engl J Med* **361:** 2019-2032.

Prentice TC and Mirand EA (1961) Effect of hypoxia on plasma erythropoietin in the rabbit. *Proc Soc Exp Biol Med* **106:** 501-502.

Provenzano R, Besarab A, Sun CH, Diamond SA, Durham JH, Cangiano JL, Aiello JR, Novak JE, Lee T, Leong R, Roberts BK, Saikali KG, Hemmerich S, Szczech LA, Yu K-HP, and Neff TB (2016a) Oral hypoxia-inducible factor prolyl hydroxylase inhibitor roxadustat (FG-4592) for the treatment of anemia in patients with CKD. *Clin J Am Soc Nephrol* **11:** 982-991.

Provenzano R, Besarab A, Wright S, Dua S, Zeig S, Nguyen P, Poole L, Saikali KG, Saha G, Hemmerich S, Szczech L, Yu K-HP, and Neff TB (2016b) Roxadustat (FG-4592) versus epoetin alfa for anemia in patients receiving maintenance hemodialysis: a phase 2, randomized, 6- to 19-week, open-label, active-comparator, dose-ranging, safety and exploratory efficacy study. *Am J Kidney Dis* **67:** 912-924.

Rankin EB, Biju MP, Liu Q, Unger TL, Rha J, Johnson RS, Simon MC, Keith B, and Haase VH (2007) Hypoxia-inducible factor-2 (HIF-2) regulates hepatic erythropoietin in vivo. *J Clin Invest* **117:** 1068-1077.

Ribeiro S, Garrido P, Fernandes J, Vala H, Rocha-Pereira P, Costa E, Belo L, Reis F, and Santos-Silva A (2016) Pathological and molecular mechanisms underlying resistance to recombinant human erythropoietin therapy in the remnant kidney rat model of chronic kidney disease associated anemia. *Biochimie* **125:** 150-162.

Rolfs A, Kvietikova I, Gassmann M, and Wenger RH (1997) Oxygen-regulated transferrin expression is mediated by hypoxia-inducible factor-1. *J Biol Chem* **272:** 20055–20062.

Sartor RB, Anderle SK, Rifai N, Goo DA, Cromartie WJ, and Schwab JH (1989) Protracted anemia associated with chronic, relapsing systemic inflammation induced by arthropathic peptidoglycan-polysaccharide polymers in rats. *Infect Immun* **57:** 1177-1185.

Seeley TW, Sternlicht MD, Klaus SJ, Neff TB and Liu DY (2017) Induction of erythropoiesis by hypoxia-inducible factor prolyl hydroxylase inhibitors without promotion of tumor initiation, progression, or metastasis in a VEGF-sensitive model of spontaneous breast cancer. *Hypoxia* **5**:1-9.

Semenza GL and Wang GL (1992) A nuclear factor induced by hypoxia via de novo protein synthesis binds to the human erythropoietin gene enhancer at a site required for transcriptional activation. *Mol Cell Biol* **12:** 5447–5454.

Shah YM, Matsubara T, Ito S, Yim S-H, and Gonzalez FJ (2009) Intestinal hypoxia-inducible transcription factors are essential for iron absorption following iron deficiency. *Cell Metab* **9:** 152–164.

Stauffer ME and Fan T (2014) Prevalence of anemia in chronic kidney disease in the United States. *PLoS ONE* doi:10.1371/journal.pone.0084943.

Szczech LA, Barnhart HX, Inrig JK, Reddan DN, Sapp S, Califf RM, Patel UD, and Singh AK (2008) Secondary analysis of the CHOIR trial epoetin-α dose and achieved hemoglobin outcomes. *Kidney Int* **74:** 791-798.

Tacchini L, Bianchi L, Bernelli-Zazzera A, and Cairo G (1999) Transferrin receptor induction by hypoxia. HIF-1-mediated transcriptional activation and cell-specific post-transcriptional regulation. *J Biol Chem* **274:** 24142–24146.

Thomas R, Kanso A, and Sedor JR (2008) Chronic kidney disease and its complications. *Prim Care* **35:** 329-344.

Thorp ML, Johnson ES, Yang X, Petrik AF, Platt R, and Smith DH (2009) Effect of anaemia on mortality, cardiovascular hospitalizations and end-stage renal disease among patients with chronic kidney disease. *Nephrology (Carlton)* **14:** 240-246.

Tian H, McKnight SL, and Russell DW (1997) Endothelial PAS domain protein 1 (EPAS1), a transcription factor selectively expressed in endothelial cells. *Genes Dev* **11:** 72-82.

Wang GL and Semenza GL (1995) Purification and characterization of hypoxia-inducible factor 1. *J Biol Chem* **270:** 1230–1237.

Wang GL, Jiang BH, Rue EA, and Semenza GL (1995) Hypoxia-inducible factor 1 is a basic-helix-loop-helix-PAS heterodimer regulated by cellular O2 tension. *Proc Natl Acad Sci U S A* **92:** 5510-5514.

Yeh T-L, Leissing TM, Abboud MI, Thinnes CC, Atasoylu O, Holt-Martyn JP, Zhang D,
Tumber A, Lippl K, Lohans CT, Leung IKH, Morcrette H, Clifton IJ, Claridge
TDW, Kawamura A, Flashman E, Lu X, Ratcliffe PJ, Chowdhury R, Pugh CW,
and Schofield CJ (2017) Molecular and cellular mechanisms of HIF prolyl
hydroxylase inhibitors in clinical trials. *Chem Sci* **8:** 7651-7668.

Yilmaz MI, Solak Y, Covic A, Goldsmith D, and Kanbay M (2011) Renal anemia of
inflammation: the name is self-explanatory. *Blood Purif* **32:** 220-225.

Zhang JH, Qi RC, Chen T, Chung TD, Stern AM, Hollis GF, Copeland RA, and
Oldenburg KR (1999) Development of a carbon dioxide-capture assay in
microtiter plate for aspartyl-beta-hydroxylase. *Anal Biochem* **271:** 137-142.

Zhang F-L, Shen G-M, Liu X-L, Wang F, Zhao H-L, Yu J, and Zhang J-W (2011)
Hypoxic induction of human erythroid-specific δ-aminolevulinate synthase
mediated by hypoxia-inducible factor 1. *Biochemistry* **50:** 1194-1202.

Footnotes

Figure Legends

Fig. 1. In vitro accumulation of HIF-1α and HIF-2α proteins by roxadustat. (A) Western blot of HIF-1α and HIF-2α in Hep3B and HK-2 cells 3 hours after exposure to either DMSO or increasing concentrations of roxadustat. (B) Western blot of HIF-α in Hep3B cells treated with DMSO or 30 µM roxadustat for 3 hours and then harvested immediately (0 minutes) or after a washout period of 15, 30, or 60 minutes.

Fig. 2. Erythropoietin (EPO) production in Hep3B cells treated with roxadustat and inflammatory cytokines. (A–C) EPO levels in the media of Hep3B cells treated with increasing concentrations of roxadustat (A), TNFα (B), or IL-1ß (C) for 72 hours. (D–E) EPO levels in the media of Hep3B cells treated with increasing concentrations of roxadustat in the presence of 0.125 ng/mL TNFα (D) or 0.125 ng/mL IL-1ß (E). Data are presented as mean ± SD. $*P < 0.05$, $**P < 0.01$, $***P < 0.001$ vs vehicle group (vs vehicle plus cytokine group for 2D & 2E).

Fig. 3. Plasma roxadustat and erythropoietin (EPO) concentrations in normal rats after a single 30 mg/kg oral dose ($n = 3$). Data are presented as mean ± S.E.M.

Fig. 4. Blood hemoglobin (Hb) concentration, hematocrit, reticulocytes, and plasma erythropoietin (EPO) concentration in normal rats treated with roxadustat three times per week for 29 days ($n = 8$ per group). EPO concentration was measured 6 hours after the final dose. Data are presented as mean ± S.E.M. $*P < 0.05$ vs vehicle group.

Fig. 5. Blood hemoglobin (Hb) concentration and red blood cell (RBC) count in cynomolgus monkeys treated with roxadustat three times per week for 52 weeks ($n = 10$ per group). Data are presented as mean ± S.E.M. *$P < 0.05$ vs vehicle group.

Fig. 6. Blood hemoglobin (Hb) concentration, hematocrit, and red blood cell (RBC) count in rats after 5/6th nephrectomy (Nx) or sham surgery and treatment with roxadustat ($n = 8$-9 per group). Treatment (5 doses over 2 weeks) was initiated 5 weeks after surgery. Data are presented as mean ± S.E.M. *$P < 0.05$.

Fig. 7. Blood hemoglobin (Hb) concentration, mean corpuscular volume (MCV), and mean corpuscular hemoglobin concentration (MCHC) in animals challenged with PG-PS ($n = 7$–8) and unchallenged (sham; $n = 4$) animals treated with vehicle, 30 mg/kg roxadustat 3 times per week, darbepoetin alpha (30 µg/kg every other week), or intravenous (IV) iron (1.5 mg/kg once per week). Treatment began 4 weeks after the PG-PS challenge and lasted for 4 weeks. Data are presented as mean ± S.E.M. *$P < 0.05$ vs corresponding (PG-PS-challenged or sham) vehicle group at the same time point.

Fig. 8. Serum iron concentration, transferrin saturation, and total iron–binding capacity, in PG-PS-challenged animals after 4 weeks of treatment with vehicle, 30 mg/kg roxadustat 3 times per week, darbepoetin alpha (30 µg/kg every other week), or intravenous (IV) iron (1.5 mg/kg once per week) ($n = 7$–8). All treatments were initiated 4 weeks after the PG-PS challenge. Sham (PG-PS-unchallenged) animals treated with

52

vehicle are also plotted for comparison ($n = 4$). Data are presented as mean ± S.E.M. *P < 0.05 vs PG-PS Vehicle group.

Fig. 9. mRNA expression of hepcidin (*Hamp*) in liver, and of iron transporter *Dmt1* (*Slc11a2*) and duodenal cytochrome b (*Dcytb*) in duodenum of PG-PS-challenged animals after 4 weeks of treatment with vehicle, 30 mg/kg roxadustat 3 times per week, darbepoetin alpha (30 µg/kg every other week), or intravenous (IV) iron (1.5 mg/kg once per week) ($n = 6$–8). All treatments were initiated 4 weeks after the PG-PS challenge. Gene expression normalized to 18S ribosomal RNA is presented as fold-change vs. vehicle group, mean ± S.E.M. *P < 0.05 vs Vehicle group.

Table 1 Summary of the pharmacokinetics of roxadustat

Species	CL (mL/hr/kg)	Vdss (mL/kg)	T1/2 (hr)	Oral F (%)
Rat [a]	33.7 ± 2.7	178 ± 19	3.6 ± 1.4	100
Monkey [b]	55.7 ± 12.2	134 ± 32	10.8 ± 1.3	70 ± 17

mean ± SD (if available)
[a] 20 mg/kg dose, n=4 (male)/group, oral F from non-crossover design
[b] 30 mg/kg dose, n=6 (3 males and 3 females)/group, oral F from crossover design

Figure 1

55
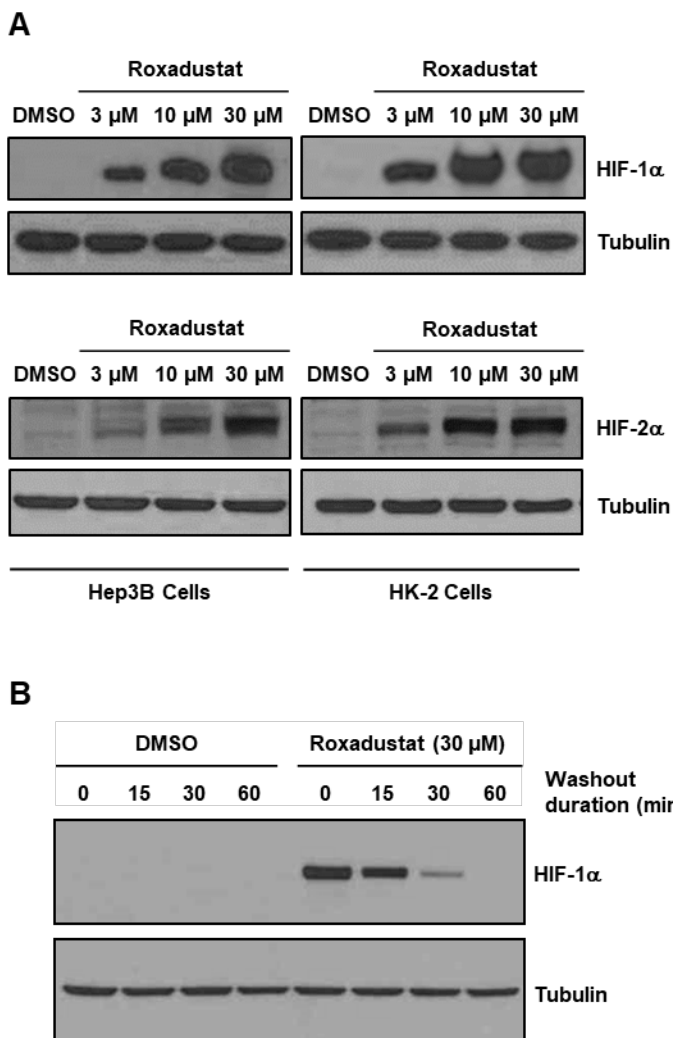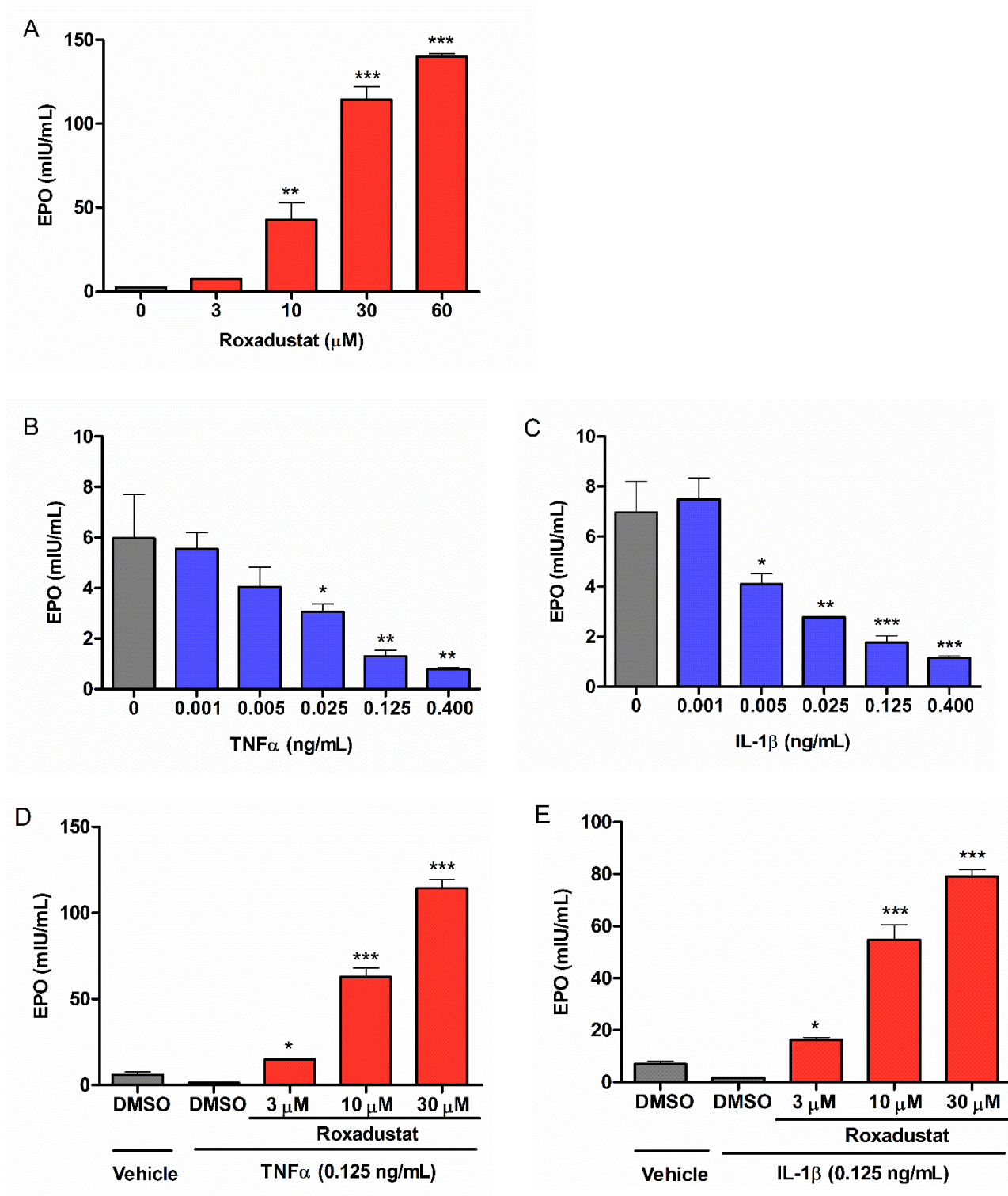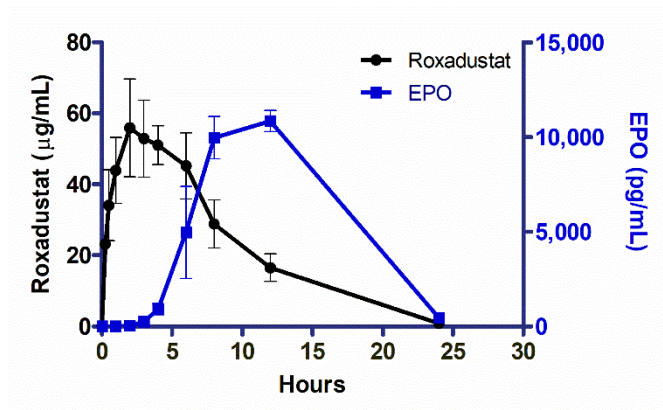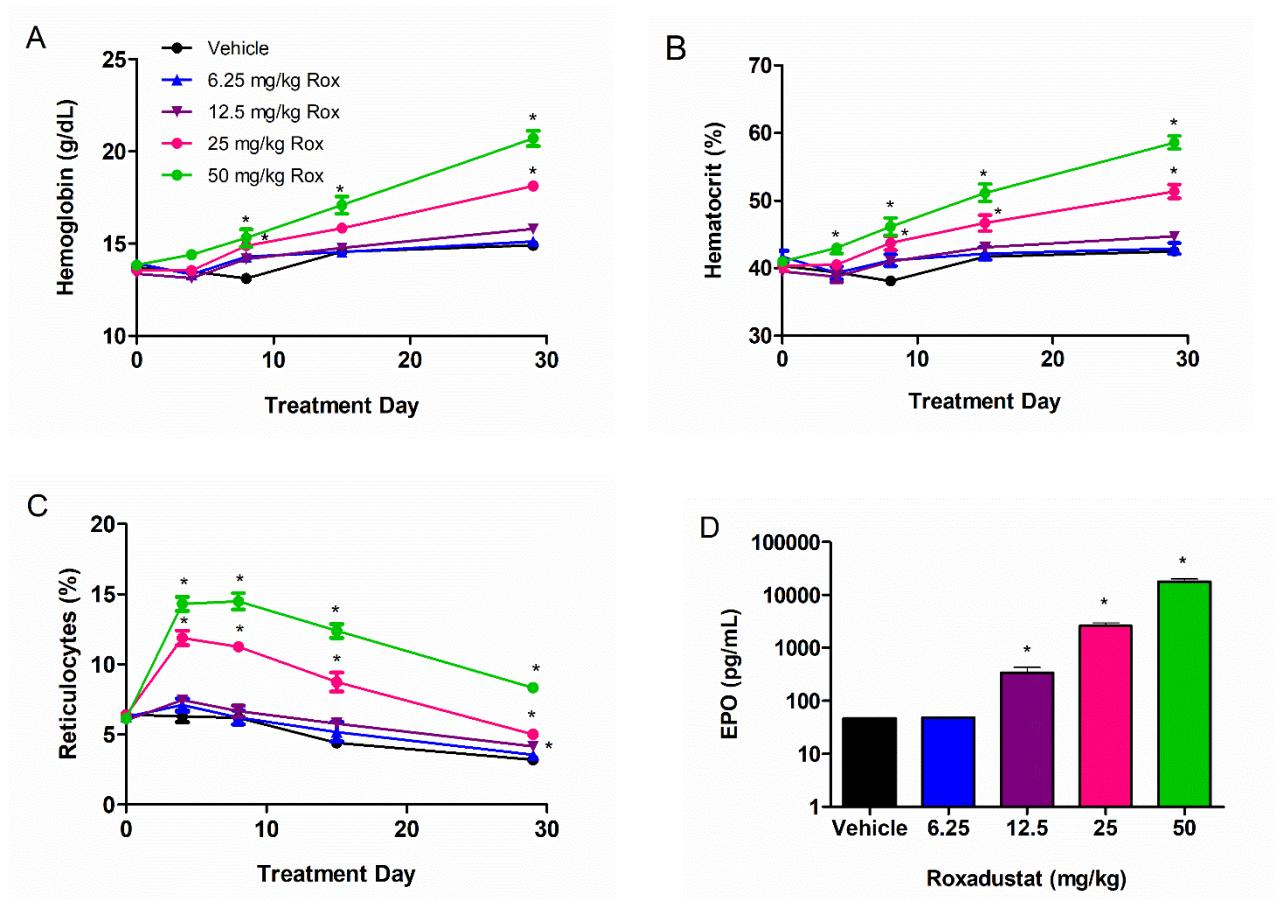
Figure 2

Figure 3

Figure 4
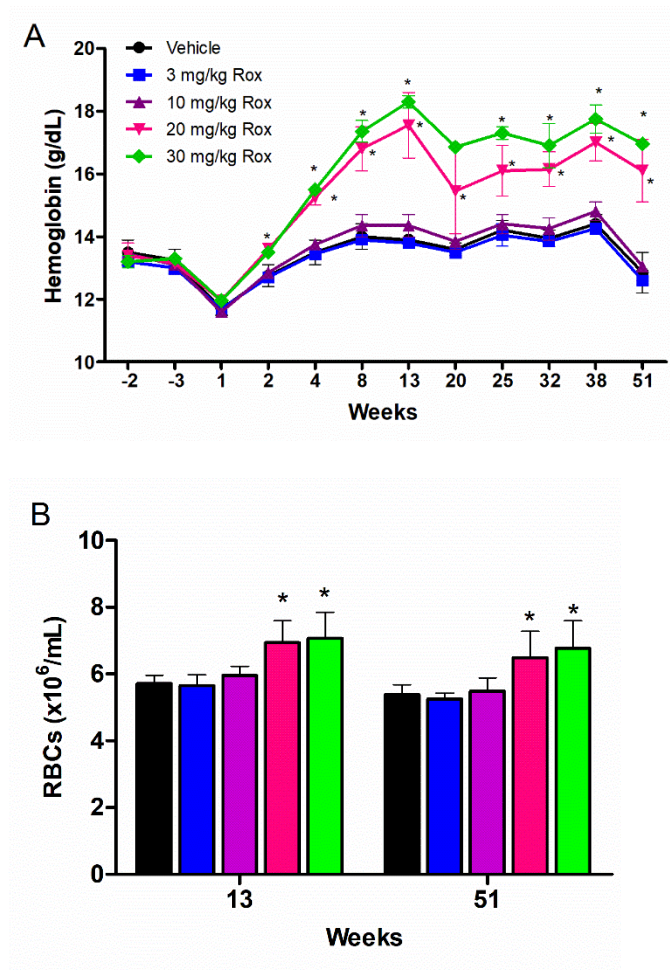
Figure 5
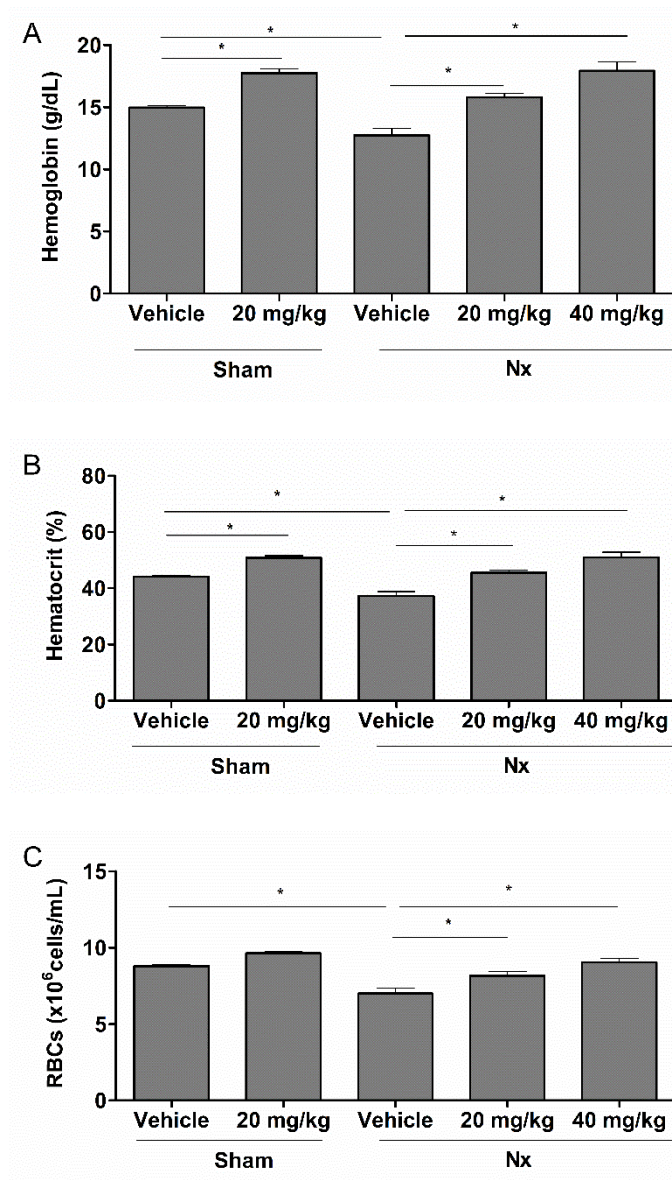
Figure 6

Figure 7

Figure 8

A

B

C
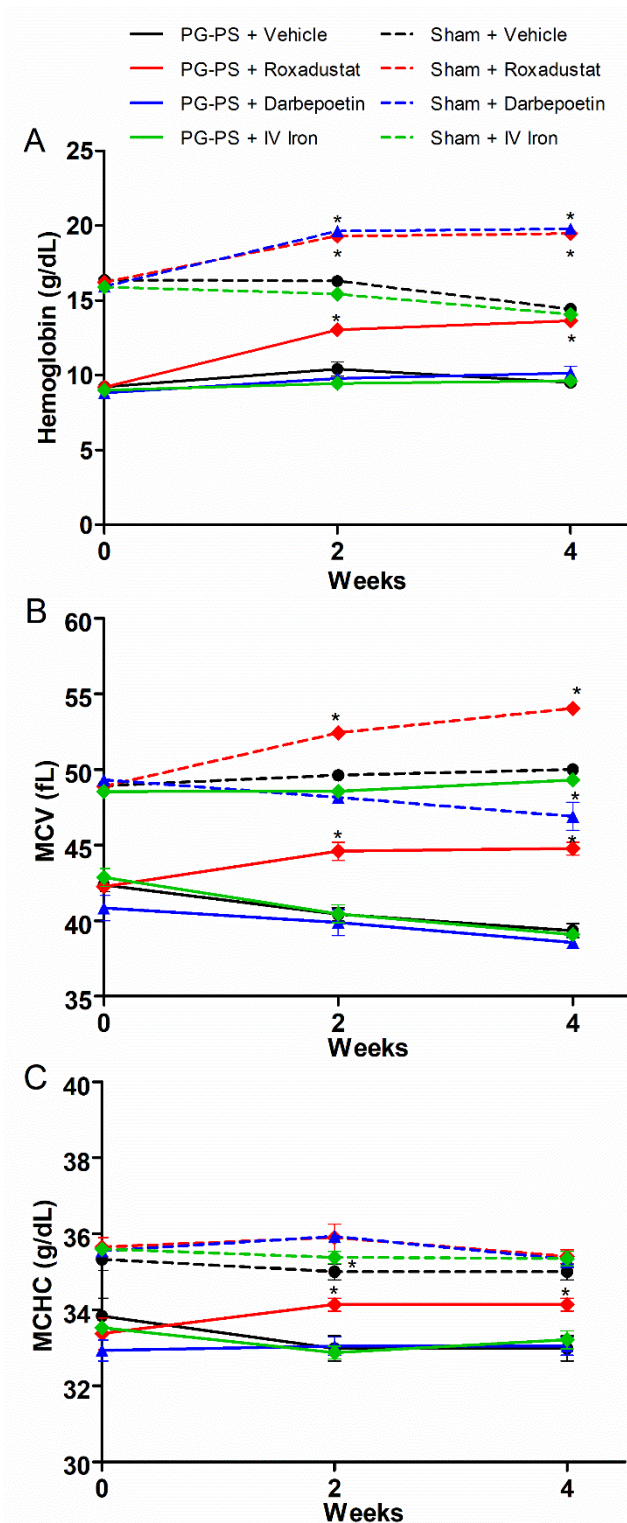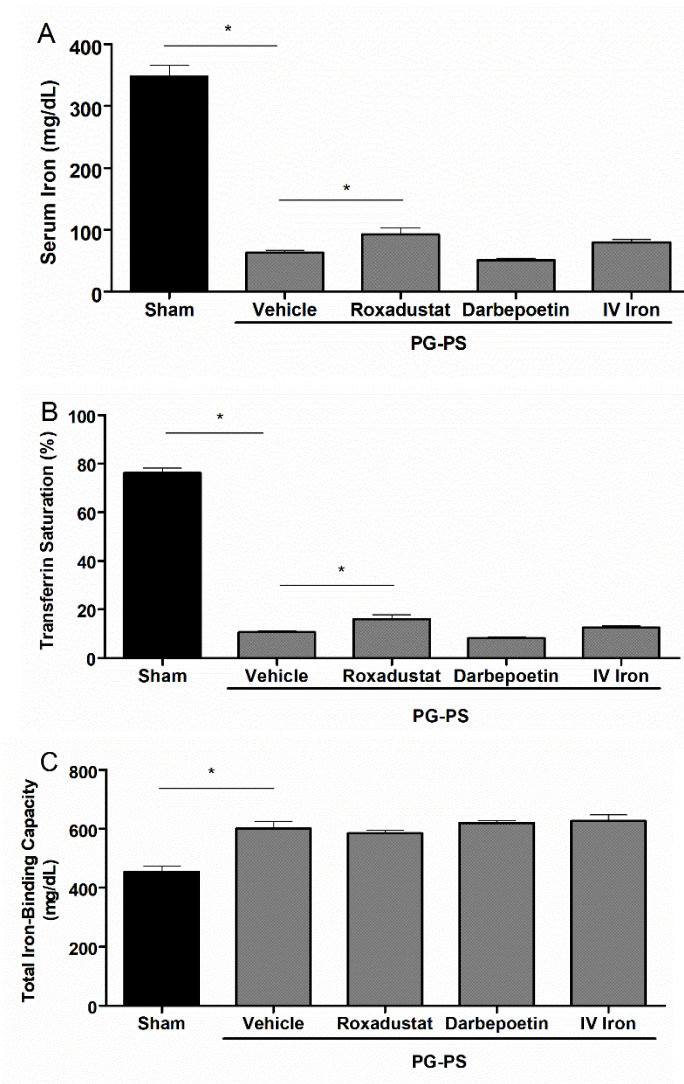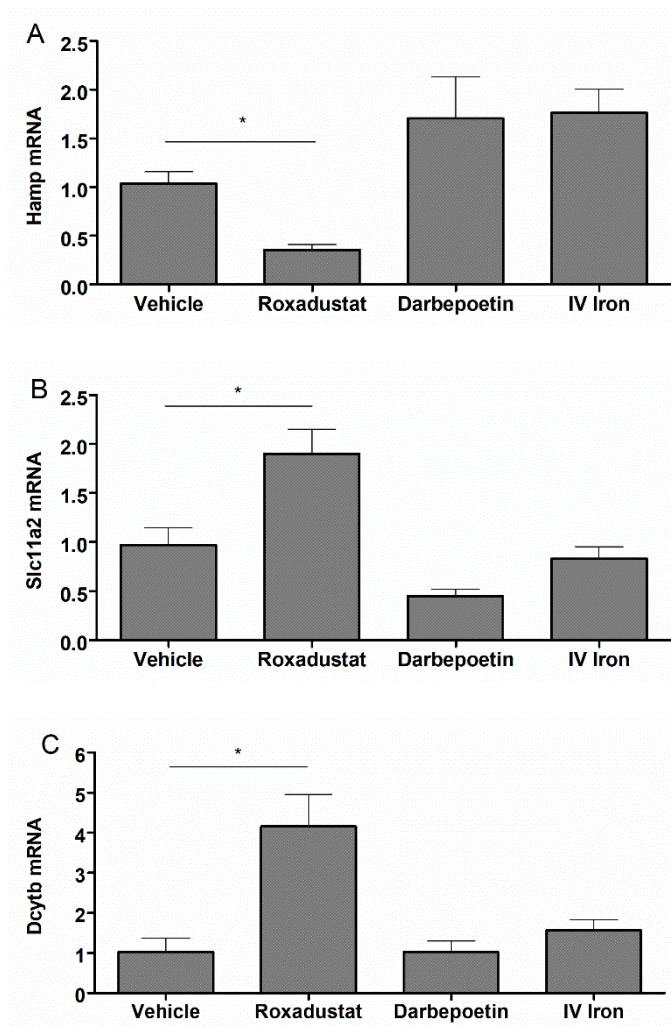
Figure 9

Nonclinical Characterization of the HIF-Prolyl Hydroxylase Inhibitor Roxadustat, a Novel Treatment for Anemia of Chronic Kidney Disease

Ughetta del Balzo, Pierre E. Signore, Gail Walkinshaw, Todd W. Seeley, Mitchell C. Brenner, Qingjian Wang, Guangjie Guo, Michael P. Arend, Lee A. Flippin, F. Aisha Chow, David C. Gervasi, Christian H. Kjaergaard, Ingrid Langsetmo, Volkmar Guenzler, David Y. Liu, Steve J. Klaus, Al Lin, and Thomas B. Neff.

Journal of Pharmacology and Experimental Therapeutics

Supplementary Fig 1. Double-reciprocal plots generated from the $V_{max,\ apparent}$ and $K_{m,apparent}$ for PHD2 (Supplementary Table 1) determined by non-linear fitting to the Michaelis-Menten equation at varying concentrations of roxadustat. Individual double-reciprocal data points are also shown. The similar intercept and increasing gradient with increasing roxadustat concentration indicates competitive inhibition with respect to αKG.

Supplementary Fig 2. Quantification of HIF western blots. HIF-α/tubulin levels are normalized to the 30 μM roxadustat condition (A, B) or the 30 μM roxadustat, 0 min condition (C).

Supplementary Fig 3. Circulating blood urea nitrogen (BUN) and serum creatinine after 5/6th nephrectomy (Nx) or sham surgery and treatment with roxadustat (n= 7-9 per group). Treatment (5 doses over 2 weeks) was initiated 5 weeks after surgery. Data are presented as mean ± S.E.M. *$P < 0.05$.

Supplementary Fig 4. Circulating white blood cell and monocyte counts, paw weight, and serum IL-6 and MIP-3α concentrations in PG-PS-challenged animals after 4 weeks of treatment with vehicle, 30 mg/kg roxadustat three times per week, darbepoetin alpha (30 μg/kg every other week), or intravenous (IV) iron (1.5 mg/kg once per week) ($n = 7$–8). All treatments began 4 weeks after the PG-PS challenge. Sham (PG-PS-unchallenged) animals treated with vehicle are also plotted for comparison ($n = 4$), except for IL-6 and MIP-3a, because cytokine levels were below the level of quantitation in unchallenged animals. Data are presented as mean ± S.E.M. *$P < 0.05$.

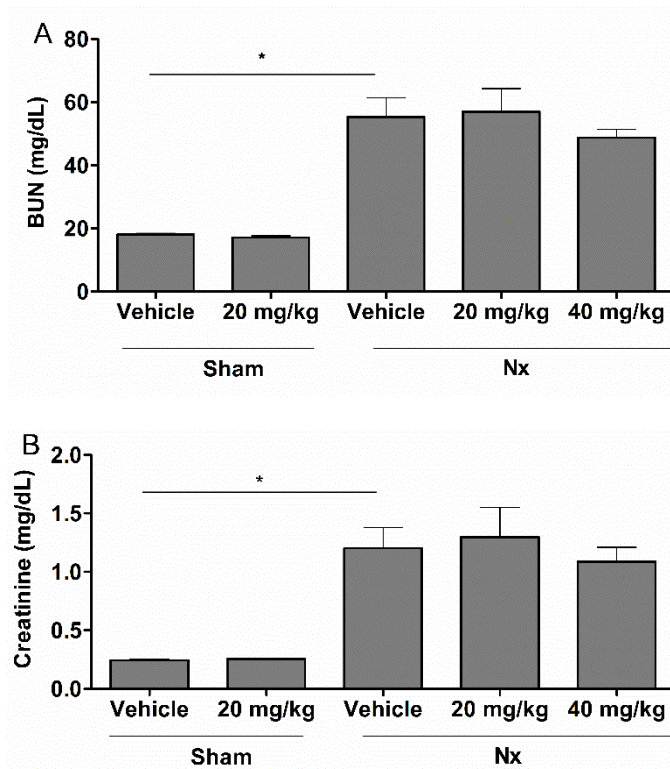**Supplementary Table 1.** Kinetic parameters for PHD2 ($K_{m,\ apparent}$ for αKG and $V_{max,\ apparent}$) obtained from non-linear best fits to the Michaelis-Menten equation at various roxadustat concentrations.
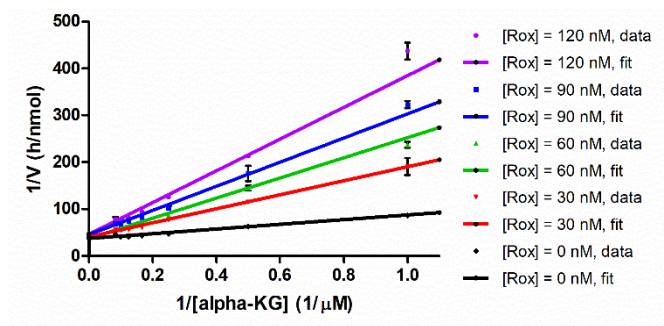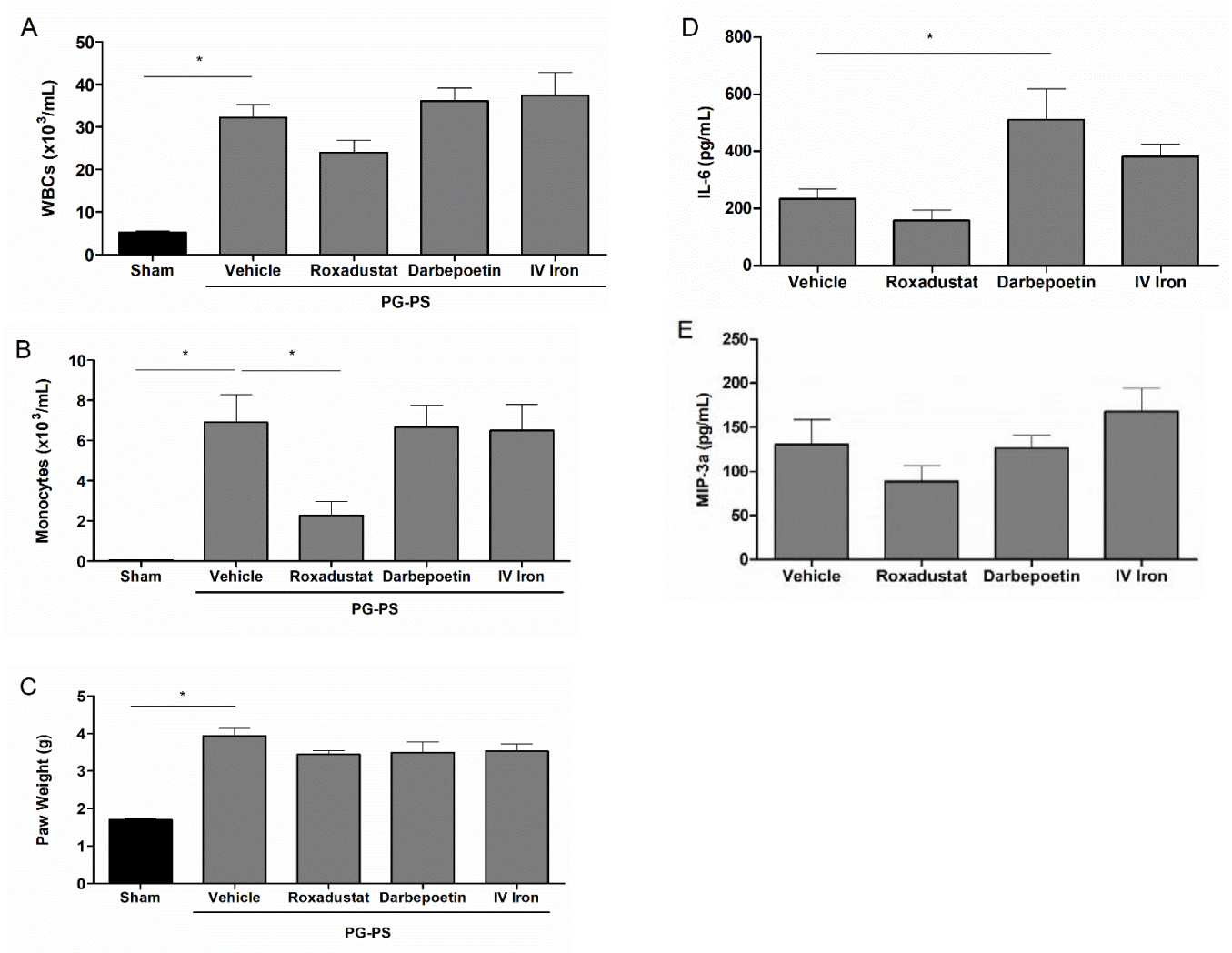
Supplementary Figure 1
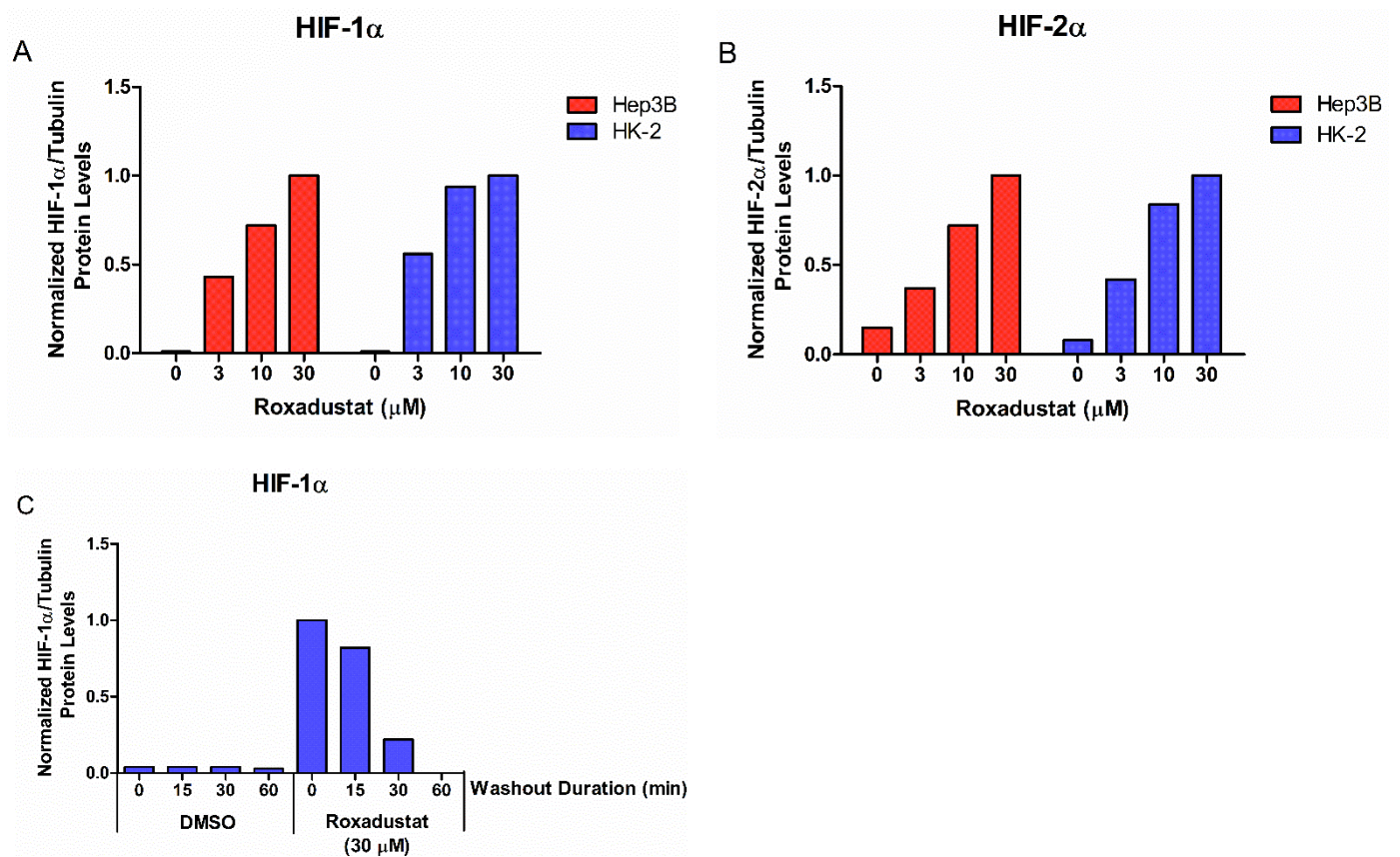
Supplementary Figure 2

Supplementary Figure 3

Supplementary Figure 4

Supplementary Table 1

[Roxadustat] (nM)	$K_{m, apparent}$ (µM) (mean ± SE)	$V_{max, apparent}$ (nmol/h) (mean ± SE)
0	1.24 ± 0.26	0.027 ± 0.0012
30	3.32 ± 0.61	0.024 ± 0.0013
60	5.18 ± 0.46	0.026 + 0.0010
90	5.17 ± 0.85	0.022 ± 0.0015
120	6.66 ± 1.42	0.022 ± 0.0022